JACS
JOURNAL OF THE AMERICAN CHEMICAL SOCIETY
pubs.acs.org/JACS
Perspective

Molecular Pumps and Motors

Yuanning Feng, Marco Ovalle, James S. W. Seale, Christopher K. Lee, Dong Jun Kim, R. Dean Astumian,* and J. Fraser Stoddart*

Cite This: *J. Am. Chem. Soc.* 2021, 143, 5569−5591

Read Online

ACCESS | Metrics & More | Article Recommendations

ABSTRACT: Pumps and motors are essential components of the world as we know it. From the complex proteins that sustain our cells, to the mechanical marvels that power industries, much we take for granted is only possible because of pumps and motors. Although molecular pumps and motors have supported life for eons, it is only recently that chemists have made progress toward designing and building artificial forms of the microscopic machinery present in nature. The advent of artificial molecular machines has granted scientists an unprecedented level of control over the relative motion of components of molecules through the development of kinetically controlled, away-from-thermodynamic equilibrium chemistry. We outline the history of pumps and motors, focusing specifically on the innovations that enable the design and synthesis of the artificial molecular machines central to this Perspective. A key insight connecting biomolecular and artificial molecular machines is that the physical motions by which these machines carry out their function are unambiguously in mechanical equilibrium at every instant. The operation of molecular motors and pumps can be described by trajectory thermodynamics, a theory based on the work of Onsager, which is grounded on the firm foundation of the principle of microscopic reversibility. Free energy derived from thermodynamically non-equilibrium reactions kinetically favors some reaction pathways over others. By designing molecules with kinetic asymmetry, one can engineer potential landscapes to harness external energy to drive the formation and maintenance of geometries of component parts of molecules away-from-equilibrium, that would be impossible to achieve by standard synthetic approaches.

■ INTRODUCTION

Modern society is built on a vast array of machines, with two of the most important being the pump and the motor. Pumps are among humanity's oldest machines, with a history[1] dating back at least 5000 years. Although man-made motors are a more recent arrival on the scene, they have become the most widely used machines today, accounting for a large fraction of global energy consumption.[2] Individually, and often in tandem, mechanical pumps and motors are the foundation for many industries and conveniences of modern life.

Pumps and motors are also ubiquitous in biological systems. In the broadest sense, from planetary atmospheric regulation,[3] to the inside of every cell in our bodies, the Earth's biosphere is driven by pumps. Biomolecular pumps and motors feature[4] prominently in all living systems and are responsible for everything from DNA transcription and membrane transport to muscle expansion and contraction. These biological machines[5,6] are highly evolved and are among the most efficient energy conversion systems. Drawing inspiration from mechanical and biological pumps and motors, scientists[7−10] have designed and synthesized artificial molecular counterparts.

In the macroscopic world, motors are, for the most part, devices that effect translation or rotation, while pumps move fluid from one place to another. Distinguishing the two is relatively simple—a motor (think of a car) moves along with what is being transported, whereas a pump remains stationary while transporting fluid. At the molecular level, however, there is no meaningful distinction. For example, DNA polymerase uses energy from the condensation of a nucleotide base to translate along single-stranded DNA by a sequence of conformational changes, leaving behind double-stranded DNA. If the polymerase is immobilized at a surface[11] however, the same sequence of shape changes[12] by which it normally translates in space, results in pumping of fluid, a reciprocal behavior which is a reflection of the Curie principle.[13]

Because of omnipresent thermal noise,[14] controlling molecular motion[15,16] is challenging. Several approaches[14] to the introduction of the energy necessary for achieving unidirectional motion have emerged. One approach employs light[17] as the energy source, while another is based on chemical fuels, and a third uses electrochemistry. On the nanoscale level, the fundamental principle of harnessing light energy to drive motion is different from the principle by which thermal or electrochemical catalysis of the degradation of a fuel molecule occurs. Ultimately this difference arises from the different constraints on the rate constants for the transitions. Rate constants for optical transitions are governed by the Einstein relations[18] whereas those for thermally activated processes, including catalyzed reactions, are governed by microscopic reversibility.[19,20] Both optical and (electro)chemical processes

Received: December 28, 2020
Published: April 8, 2021

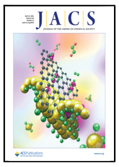

Downloaded via UNIV OF CALIFORNIA SANTA BARBARA on May 15, 2021 at 19:25:58 (UTC).
See https://pubs.acs.org/sharingguidelines for options on how to legitimately share published articles.

ACS Publications

https://doi.org/10.1021/jacs.0c13388

obey a principle described as "detailed balance" at equilibrium, according to which every process is as likely as the exact reverse of the process. This principle is often incorrectly described as being synonymous with microscopic reversibility. Detailed balance is instead a corollary—valid only at equilibrium—of both the Einstein relations[18] and of microscopic reversibility.[19,20]

In addition to choosing an energy source, artificial molecular machines (AMMs) must be designed creatively to harvest energy input. A number of research groups have adopted their own unique approaches, but all share the breaking of symmetry as an essential requirement. Mechanical bonds,[9,10,16,21−23] which define mechanically interlocked molecules[8,9] (MIMs), have provided one solution for crafting AMMs. MIMs are molecules composed of component parts that cannot be separated without breaking constitutive covalent or coordinative bonds. While separation of the constituent parts is prevented, relative motion between the components of MIMs is still possible. The incorporation of molecular recognition sites and steric barriers into these molecules allows the relative motions of the component parts to be controlled by external stimuli, thus enabling the creation of AMMs, including pumps and motors. The controlled, unidirectional motion that these pumps and motors exhibit allows an unprecedented level of control at the molecular level. While we can only speculate on the potential applications of AMMs, it is clear that the age of artificial molecular machines[7−10,16,23] is now dawning.

■ MAN-MADE MACROSCOPIC PUMPS AND MOTORS

Two of the most important mechanical devices that power the modern world are the pump and the motor. Pumps are among the oldest known machines while motors are a relatively recent development. Although electric motors first appeared[24] in the early part of 19th century, they did not come into general use until half-a-century later. Nowadays, they are of central importance in modern society. Let us examine some of the principles of macroscopic pumps and motors in order to facilitate our later discussion of artificial molecular machines.

Fundamentally, pumps and motors are energy conversion systems. While motors[2,24] convert electrical to mechanical energy, pumps[1,25] use mechanical work to increase fluid energy. On account of their long history, pumps have many different designs. They can be categorized[26] by operational principles into three major classes—dynamic, direct lift, and positive displacement pumps. Dynamic pumps function by the continuous addition of kinetic energy to a fluid. This category is by far the most prevalent since it includes centrifugal pumps, which alone account[26] for 80% of all pumps. Direct-lift devices, including the earliest pumps, operate by containing and physically elevating a fluid. Positive displacement pumps enclose fixed volumes of fluid and mechanically move this volume through a system. In a chemistry laboratory setting, syringe and peristaltic pumps are common examples of positive displacement pumps. These different types of pumps are customized for different applications and, in combination, they are used in almost every industry.

All electric motors operate by electromagnetic induction. They are constructed (Figure 1) of two main assemblies—(i)[24] the rotor, which consists of all rotating components, and (ii) the stator, which consists of all stationary components. These motors can be constructed in a wide range of sizes and are used in everything from household appliances to the largest industrial machines.

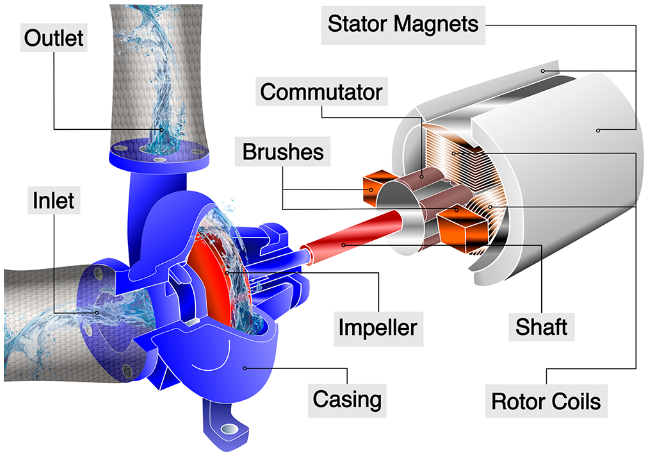

Figure 1. A centrifugal mechanical pump (blue), driven by an electric motor (gray). The brushes are stationary and transmit power to the rotor by way of the commutator. The commutator inside the electric motor transmits this electrical power to an individual set of rotor coils, producing a magnetic field by electromagnetic induction. This induced field attracts and repels the magnets selectively in the stator, producing electromotive force and generating torque, resulting in the rotation of the rotor. As the rotor turns the commutator transfers power to the successive sets of rotor coils thus creating continuous rotation. The generated torque is transferred along the shaft of the motor to turning the impeller of the pump. As the impeller gains velocity, it imparts kinetic energy to the fluid at the inlet, driving it to a higher energy. The fluid, now at elevated pressure, flows through the casing of the pump and is released at the outlet.

Pumps and motors are usually associated with man-made machines that operate mechanically. This idea, however, is far from the whole truth. Such devices are not just limited to the man-made world but are, in fact, vital components of the human body as well. Pumps in particular are ubiquitous in nature at all scales, from the macroscopic oceanic biological pump[3,27] to the biomolecular pumps inside of our cells.[28,29]

■ BIOMOLECULAR PUMPS AND MOTORS

Let us take a fantastic voyage,[30] à la Mr. Tompkins, viewing the world through the eyes of a molecular machine. The first thing that we would notice would be the enormous pelting received by water molecules, where the ratio of size between water and the machine is similar to that between a hailstone and a car.[31] These many collisions have given rise to the description of molecular machines as "walking in a hurricane"[14] and result in the phenomenon of Brownian motion, or in aggregate, of diffusion. Every collision influences the different bonds in the machine differently, but because of the staggering number of collisions[32] ($\sim 10^{20}$ s^{-1}), each bond maintains the average kinetic energy, $\frac{1}{2}k_BT$, even on short time scales. This result is known as the equipartition theorem[33,34] which states that any imbalance of kinetic energy among different degrees of freedom vanishes on short (<ps) time scales. Without a heat source, a molecular machine is in thermal equilibrium at every instant.

The circumstance in which viscous drag is far more important than inertia, as is the case with all molecular machines in solution, is known as the low Reynolds number regime as described beautifully by Purcell.[35] Because in this regime the viscous drag force is equal and opposite to the inertial force at every instant,[36] there is no acceleration; hence, molecular machines carry out their function by mechanically equilibrated motions, and any directionality requires a non-reciprocal sequence of conformational changes that can be thought of as swimming in molasses.[14]

The disequilibrium that allows for directed motion arises from the fact that the chemical potentials of some components are different from the chemical potentials of other components. The direction in which thermodynamic disequilibrium[37] drives motion, whether translation, rotation, or pumping, is governed solely by the kinetic asymmetry[38] of the system.

Pumps have typically been treated very differently than motors in the biochemical and biophysical literature.[39−41] The standard picture of an ion pump invokes a model where a protein embedded in a bilayer membrane undergoes conformational changes by which an ion-binding site switches between facing the inside and facing the outside of a cell. This conformational switching is controlled by phosphorylation/dephosphorylation during ATP hydrolysis. In contrast, motors are often viewed by many in the field[42,43] in terms of an ATP-driven "power-stroke" (PS)—a large-amplitude, energetically downhill, conformational change that "generates force" and hence allows molecular motors to do work against an applied force. As we compare and contrast a molecular pump (Ca^{2+} ATPase) with a molecular motor—myosin moving on actin—we come to realize that the mechanistic distinction between these two classes of molecular machines is non-existent. In fact, all catalysis-driven pumps and motors work by a mechanism similar to the alternating-access model that can be termed an information ratchet.[5,38,44,45]

Biomolecular Pumps. At the nanoscale level pumps are a part of every organism, where their primary role[4] is to effect the membrane transport of, for example, ions, amino acids, carbohydrates, lipids, and other small molecules. The creation and maintenance of transmembrane concentration gradients and the transport of ions and neutral molecules by pumps[41] are essential for many biological processes, such as the action-potential in neurons, muscle and cardiac cells function, cellular signaling, transporting metabolites, and the selective import of nutrients and export of toxins through cell walls. Primary transport membrane ion pumps use different sources of energy to generate electrochemical gradients. Secondary transport membrane pumps use these electrochemical gradients to transport ions and other small molecules across membranes.[46]

Now let us consider P-Type ATPases,[47] a specific type of transport membrane pump that involves ATP-meditated phosphorylation/dephosphorylation, which function by an alternating-access mechanism known as the E_1−E_2 Post-Albers model.[48] A classic example is the Na^+, K^+ ATPase which was first described by Skou[49] in 1957, leading to being awarded the Nobel Prize in Chemistry[50] in 1997. For stochiometric simplicity, let us consider another P-type pump, the Ca^{2+} ATPase that transports only one ion per cycle. Phosphorylation triggers conversion from an E_1 form (Figure 2a, left), with its ion-binding site facing one side of the membrane, and an E_2 form (Figure 2a, right), with its ion-binding site facing the other side of the membrane. This pump is perhaps the most and best studied of the P-Type enzymes[51] because of its importance in muscle physiology. A kinetic mechanism for coupling ATP hydrolysis to transport is shown in Figure 2b. The mechanism is consistent with Jencks' rules[52] for vectorial coupling in which ion-binding/release steps, phosphorylation/dephosphorylation steps, and conformational changes are interleaved. This interleaving can be also described as an escapement mechanism as discussed by Branscomb[36,53] and Carter.[54,55] Every completion of a cycle (Figure 2b) $1\rightarrow2\rightarrow3\rightarrow4\rightarrow1$ is accompanied by transport from the cytosol to the lumen. Conversely, every completion of a cycle $1\rightarrow4\rightarrow3\rightarrow2\rightarrow1$ is accompanied by transport from the lumen to the cytosol.

It is common but very misleading to show only the top reaction in the ATP hydrolysis steps. This mistaken representation was derisively termed by Koenig, Horne, and Mohilner[56] as "coupling by the stroke of a pen" because the predicted direction of ATP hydrolysis-coupled ion flow depends solely on the researcher's choice of whether to select the top reactions (Figure 2b, top arrows $2\rightleftharpoons2^P$ and $4\rightleftharpoons4^P$), in which the ATP hydrolysis-driven transport is from cytosol to lumen, or the bottom reactions, in which case the predicted flow is from lumen to cytosol. In either case, the essential point is that the free energy of ATP hydrolysis drives transport, but the selection between the top and bottom sets of arrows—kinetic asymmetry—determines whether the cycle $1\rightarrow2\rightarrow3\rightarrow4\rightarrow1$ (cytosol to lumen) or $1\rightarrow4\rightarrow3\rightarrow2\rightarrow1$ (lumen to cytosol) predominates.

Biomolecular Motors. Motor proteins[57] travel unidirectionally along cytoskeletal filaments while carrying out functions such as intracellular organelle transport, precise chromosome segregation during cell division, and the molecular motions necessary for muscular movements. Other biomolecular motors[58] play key roles in replication, transcription, and translation, such as the DNA and RNA polymerases,[59] which operate on a nucleic acid track in a unidirectional fashion to read or write genetic codes. Outside the cell, the underlying mechanism, by which bacterial flagella and the related cilia[60] harness chemical energy to rotate and beat to power cellular motion, follows the same principles as those operating in single biomolecular motors. Their ability, however, to achieve synchrony remains an abiding biological mystery.[60]

Molecular motors are often described very differently than are molecular pumps. Läuger,[41] in his seminal treatise "Electrogenic Ion Pumps", has pointed out explicitly that ion pumps do not function by a "power-stroke" mechanism. In contrast, molecular motors such as myosin are often described in terms of a large-amplitude, "force-generating" conformational change, known as a "power-stroke". Myosin (from Greek *mys*, muscle) was the first motor protein discovered[61] and is by far the best investigated to date. Since the discovery of myosin I by Pollard and Korn[62] in 1973, multiple forms have been identified.[61,63,64] Like the ion pumps, myosin is also an ATPase. The structure of myosin (Figure 2c) is shown in two different conformations, labeled as pre- and post-"power-stroke" states. X-ray crystallographic structures are no doubt the origin of claims concerning the "structural origins of the power-stroke" put forth recently by Hwang and Karplus.[42] Their interpretation is problematic, relying as it does on an input of energy—represented in their diagram with a lightning bolt and the words "fuel event"—to prime the molecule into a high energy form from which it can undergo relaxation in a process termed the "power-stroke", as shown on the right-hand side of Figure 2c. This picture is not consistent with the principle of microscopic reversibility[19,20] and is thermodynamically incorrect. The description is misleading especially because light-driven motors, such as rhodopsins and photosynthetic reaction centers,[65] do operate by a power-stroke mechanism

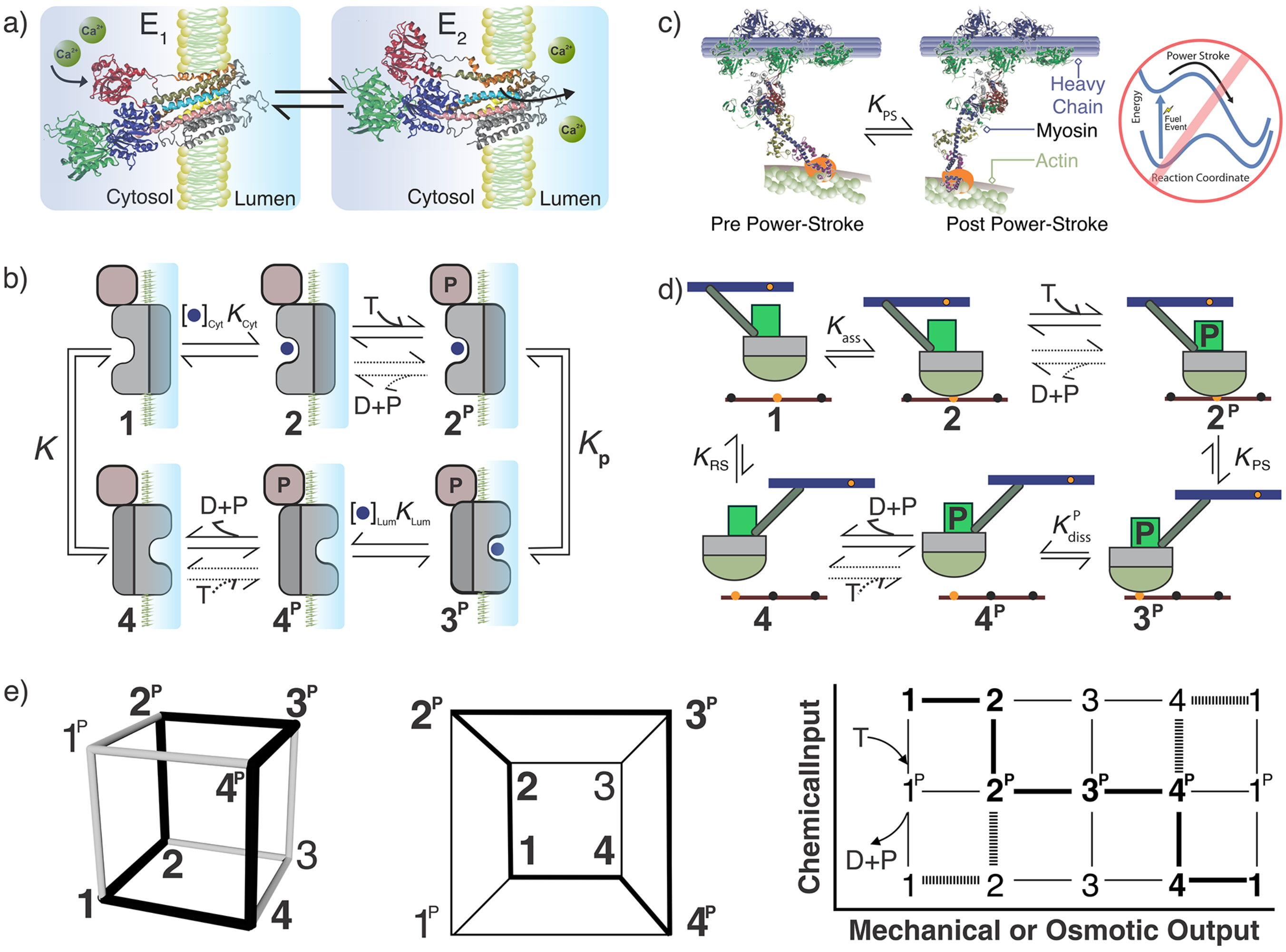

Figure 2. A comparison between biomolecular pumps and motors. (a) The Ca^{2+} ATPase pump embedded in a bilayer membrane. There are two different forms, E_1 and E_2, that differ in their access to an ion-binding site from the two sides of the membrane. In the E_1 form, the binding site is open to the cytosol, and in the E_2 form, the binding site is open to the lumen. The transitions between E_1 and E_2 occur by thermal activation. The equilibrium constant governing the conformational change is in general different when the protein is phosphorylated (K_p) than when it is not phosphorylated (K). (b) A simplified schematic kinetic mechanism for ATP hydrolysis-driven ion transport is shown as a cycle of states, where each clockwise cycle transports an ion (blue circle) from the cytosol (left) to the lumen (right), and each counterclockwise cycle transports an ion from the lumen to the cytosol. The fuel ATP is represented by T, ADP is represented by D, and inorganic phosphate, P_i, by P. The energy input comes from the tendency of ATP to be hydrolyzed rather than synthesized, a tendency that biases the direction of cycling based on the specificities for ATP versus ADP in states 2 and 4. The ratio of clockwise (cw) to counterclockwise (ccw) cycles is $\frac{\pi(\text{cw})}{\pi(\text{ccw})} = \mathcal{A}_2\mathcal{A}_4^{-1}$ [see eq 1]. Significantly, this ratio is independent of the equilibrium constants of the reactions, i.e., is independent of the free energies of the states. (c) Two crystal structures of myosin: on the left, the pre-"power-stroke" state, and on the right, the post-"power-stroke" state. The common myth invoked in the field of biomolecular machines is that the energy released, $RT \log K_{ps}$, in the transition between the two states is responsible for the ability of the system to do work against an applied load. This assertion is simply not true as shown by examining the complete kinetic cycle for the process. (d) A kinetic cycle incorporating the "power-stroke" (PS), accomplished with myosin (blue) attached to actin (green), and the "recovery-stroke" (RS), accomplished with myosin detached from actin. Completion of a clockwise cycle transports actin by the stroke distance to the left in the figure, while completion of a counterclockwise cycle transports actin by the stroke distance to the right in the figure. Despite lots of words used to elaborate the critical importance of the "power-stroke", by use of microscopic reversibility we find that, as for the aforementioned ion pump, the ratio of the probability for a clockwise to counterclockwise cycle for this motor is $\mathcal{A}_2\mathcal{A}_4^{-1}$ [see eq 1]. This ratio is independent of any equilibrium constants and is hence independent of the free energies of the states. (e) Three kinetic representations for the identical kinetic cycles of the discussed pump and motor. The hypercycle in the middle is a projection of the cube on the left onto a plane. The 2D kinetic representation on the right is slightly different: it considers the hydrolysis and the coupled process (ion transport for the pump or actin motion for the myosin motor) as separate coordinates on a 2D periodic landscape. The elaboration of the pathways in terms of the bold or dashed transitions illustrate the characteristic zigzag pattern associated with coupled transport. If state 2 is specific for T and state 4 specific for D (bold lines), the downward tendency arising from ATP hydrolysis tends to drive the system to the right. If state 2 is specific for D and state 4 is specific for T (dashed lines), the downward tendency resulting from ATP hydrolysis tends to drive the system to the left.

and are described correctly by a diagram such as the one to the right of the two structures (Figure 2c) for myosin. Light-driven processes are not constrained by microscopic reversibility[19,20] and must instead obey the Einstein relations[18] for absorption and emission of light.

A cyclic mechanism for myosin is shown in Figure 2d. As in the case of the ion pump, the lower transitions for the ATP hydrolysis are often not shown. This omission, as before, is problematic and obscures the actual mechanism by which unidirectional motion occurs in muscle.

Kinetic Asymmetry and the Mechanism of Biomolecular Pumps and Motors. The mechanisms for both the pump and the motor can be cast more generally as shown in Figure 2e. The left and center representations[66,67] are equivalent, with the center representation being a projection of the left, cube, representation in Figure 2e. These representations reflect the fact that the states of both the pump and the motor can be described in terms of three dichotomic (2×2×2) properties. For the pump, these properties are E_1 and E_2, binding site occupied and empty, and phosphorylated and dephosphorylated. For the motor, these properties are pre- and post-power-stroke, attached to and detached from actin, and phosphorylated and dephosphorylated. The ratios for the elementary rate constants for the conformational changes, $E_1 \rightleftharpoons E_2$ or pre-"power-stroke" $\rightleftharpoons$ post-"power-stroke", and for the ion-binding changes occupied $\rightleftharpoons$ empty and also attached $\rightleftharpoons$ detached, are given by microscopic reversibility[19,20] in the familiar Boltzmann form, i.e., as equilibrium constants. The transitions between phosphorylated $\rightleftarrows$ dephosphorylated are not described by elementary rate constants and their ratio is given as the product of an equilibrium constant and a kinetic asymmetry factor.[68−70]

We can see the importance of kinetic asymmetry by considering the Michaelis−Menten[71] mechanism for the catalytic process of ATP hydrolysis (Scheme 1) carried out by any of the four states:

Scheme 1

$$\mathrm{ATP} + i \underset{k_{i,\mathrm{off}}}{\overset{[\mathrm{ATP}]k_i^{\mathrm{T}}}{\rightleftharpoons}} i^{\mathrm{P}} \underset{[\mathrm{ADP}][\mathrm{P_i}]k_i^{\mathrm{D\cdot P}}}{\overset{k_{i,\mathrm{cat}}}{\rightleftharpoons}} i + \mathrm{P_i} + \mathrm{ADP} \text{ for } i = 1, 2, 3, 4$$

where $\frac{[\mathrm{ADP}][\mathrm{P_i}]k_i^{\mathrm{D\cdot P}}k_{i,\mathrm{off}}}{[\mathrm{ATP}]k_i^{\mathrm{T}}k_{i,\mathrm{cat}}} = \mathrm{e}^{-\Delta G_{\mathrm{ATP}}/RT}$. The effective transition constants for the processes $i \underset{\omega_{i,\mathrm{off}}}{\overset{\omega_{i,\mathrm{on}}}{\rightleftarrows}} i^{\mathrm{P}}$ are $\omega_{i,\mathrm{off}} = (k_{i,\mathrm{off}} + k_{i,\mathrm{cat}})$ and $\omega_{i,\mathrm{on}} = ([\mathrm{ATP}]k_i^{\mathrm{T}} + [\mathrm{ADP}][\mathrm{P}_i]k_i^{\mathrm{P}})$, and their ratio is

$$\frac{\omega_{i,\mathrm{on}}}{\omega_{i,\mathrm{off}}} = \frac{[\mathrm{ATP}]k_i^{\mathrm{T}}}{k_{i,\mathrm{off}}} \underbrace{\left[\frac{\left(\frac{k_{i,\mathrm{off}}}{k_{i,\mathrm{cat}}} + \mathrm{e}^{-\Delta G_{\mathrm{ATP}}/RT}\right)}{\left(\frac{k_{i,\mathrm{off}}}{k_{i,\mathrm{cat}}} + 1\right)}\right]}_{\mathcal{A}_i} = K_i^{\mathrm{T}}\mathcal{A}_i \tag{1}$$

where $K_i^{\mathrm{T}} = \frac{[\mathrm{ATP}]k_i^{\mathrm{T}}}{k_{i,\mathrm{off}}}$ is the binding constant for ATP, and $\mathcal{A}_i$ is a kinetic asymmetry factor[69] that describes the kinetic gating of the driving reaction. The ratio $\frac{k_{i,\mathrm{cat}}}{k_{i,\mathrm{off}}}$ parametrizes the kinetic selection between the two "off" rates from the phosphorylated state $\xleftarrow{k_{i,\mathrm{off}}} i^{\mathrm{P}} \xrightarrow{k_{i,\mathrm{cat}}}$ and does not depend on the free energies of any of the states but only on the relative energies of the transition states for dissociation to substrate or product. When $k_{i,\mathrm{off}} \gg k_{i,\mathrm{cat}}$, we say the state i is specific for substrate, and when $k_{i,\mathrm{cat}} \gg k_{i,\mathrm{off}}$, the state i is specific for product. The ratio of clockwise to counterclockwise cycles in the left and middle diagrams in Figure 2e is $r_0 = \underbrace{K_{12}K_{22^{\mathrm{P}}}K_{2^{\mathrm{P}}3^{\mathrm{P}}}K_{3^{\mathrm{P}}4^{\mathrm{P}}}K_{4^{\mathrm{P}}4}K_{41}}_{=1}\mathcal{A}_2\mathcal{A}_4^{-1}$. If $\Delta G_{\mathrm{ATP}} = 0$, both kinetic asymmetry factors are individually unity and $r = 1$, but if $\frac{k_{2,\mathrm{cat}}}{k_{2,\mathrm{off}}} = \frac{k_{4,\mathrm{cat}}}{k_{4,\mathrm{off}}}$, then $r_0 = 1$, irrespective of the value of ΔG_{ATP}. This result shows that the current emphasis on dissipation-driven processes is seriously misguided. Dissipation is, of course, an ineluctable accompaniment to directed motion, non-equilibrium assembly, and adaptation, but by no means is it sufficient. The essential design feature is kinetic asymmetry, which constrains all non-equilibrium behavior.

The panel on the right[69] of Figure 2e offers another view of how directionality is determined in molecular machines. This representation focuses on the periodicity of the overall catalytic processes, where one periodic completion in each direction is shown in the representation on the right in Figure 2e. In this representation, each forward and backward transition is characterized by a pair of elementary rate constants, and so the ratios are given by microscopic reversibility.[19,20] The key discrimination occurs at states 2 and 4. If state 2 is specific for ATP and state 4 is specific for ADP·$\mathrm{P_i}$, then the overall hydrolysis-driven mechanism proceeds from left-to-right along the bold trajectory in the order 1→2→3→4→1. If state 2 is specific for ADP·$\mathrm{P_i}$ and state 4 is specific for ATP, then the hydrolysis-driven mechanism proceeds from right-to-left along the dashed trajectory in the order 1→4→3→2→1. The energy released in steps $1 \rightleftharpoons 2$ and $3^{\mathrm{P}} \rightleftharpoons 4^{\mathrm{P}}$ play no role at all in determining the direction of motion, stopping load, or optimal efficiency.[72] The confusion in the literature about the role of the "power-stroke" seems to arise from visualizing a mechanism involving a deposition of energy and a single specific transition. While this perspective is indeed valid for light-driven processes, Hill and Eisenberg[73] have shown that energy transduction cannot be localized in a specific transition for catalysis-driven processes.

Why the Power-Stroke Model Is Wrong for Catalysis-Driven Motors. The idea behind the putative power-stroke model is very simple—chemical energy, e.g., from phosphorylation by ATP, is used to promote a motor molecule (Figure 2c) from a low free-energy state (i) into a high free-energy state (i^{P}) from which it relaxes directionally to a lower free-energy state (j^{P}). This relaxation process is called a power-stroke (PS). Spontaneous dephosphorylation resets the system to state j from which the motor can execute the recovery-stroke (RS) back to state i, but having undergone some translation or having accomplished some task by means of the directional relaxation. In order to understand why this simple and natural picture is wrong, we must view the overall process holistically—as part of a complete cycle—and not just in terms of the power-stroke. The process can be described (Scheme 2) as

Scheme 2

$$i \;\underset{\mathrm{K}_i^{\mathrm{D\cdot P}}}{\overset{\mathrm{K}_i^{\mathrm{T}}}{\begin{matrix}\rightleftharpoons\\ \rightleftharpoons\end{matrix}}}\; \underbrace{i^{\mathrm{P}} \overset{\mathrm{K}_{\mathrm{PS}}}{\rightleftharpoons} j^{\mathrm{P}}}_{\text{"power stroke"}} \;\underset{\mathrm{K}_j^{\mathrm{T}}}{\overset{\mathrm{K}_j^{\mathrm{D\cdot P}}}{\begin{matrix}\rightleftharpoons\\ \rightleftharpoons\end{matrix}}}\; \overbrace{j \rightleftharpoons \cdots \rightleftharpoons i}^{\mathrm{K}_{\mathrm{RS}}}$$

where $K_i^{\mathrm{T}} = \frac{[\mathrm{ATP}]k_i^{\mathrm{T}}}{k_{i,\mathrm{off}}}$, $K_j^{\mathrm{T}} = \frac{[\mathrm{ATP}]k_j^{\mathrm{T}}}{k_{j,\mathrm{off}}}$, $K_i^{\mathrm{D\cdot P}} = \frac{[\mathrm{ADP}][\mathrm{P_i}]k_i^{\mathrm{D\cdot P}}}{k_{i,\mathrm{cat}}}$, and $K_j^{\mathrm{D\cdot P}} = \frac{[\mathrm{ADP}][\mathrm{P_i}]k_j^{\mathrm{D\cdot P}}}{k_{j,\mathrm{cat}}}$. Each transition between the unphosphorylated and phosphorylated states can occur by one of two paths, one path

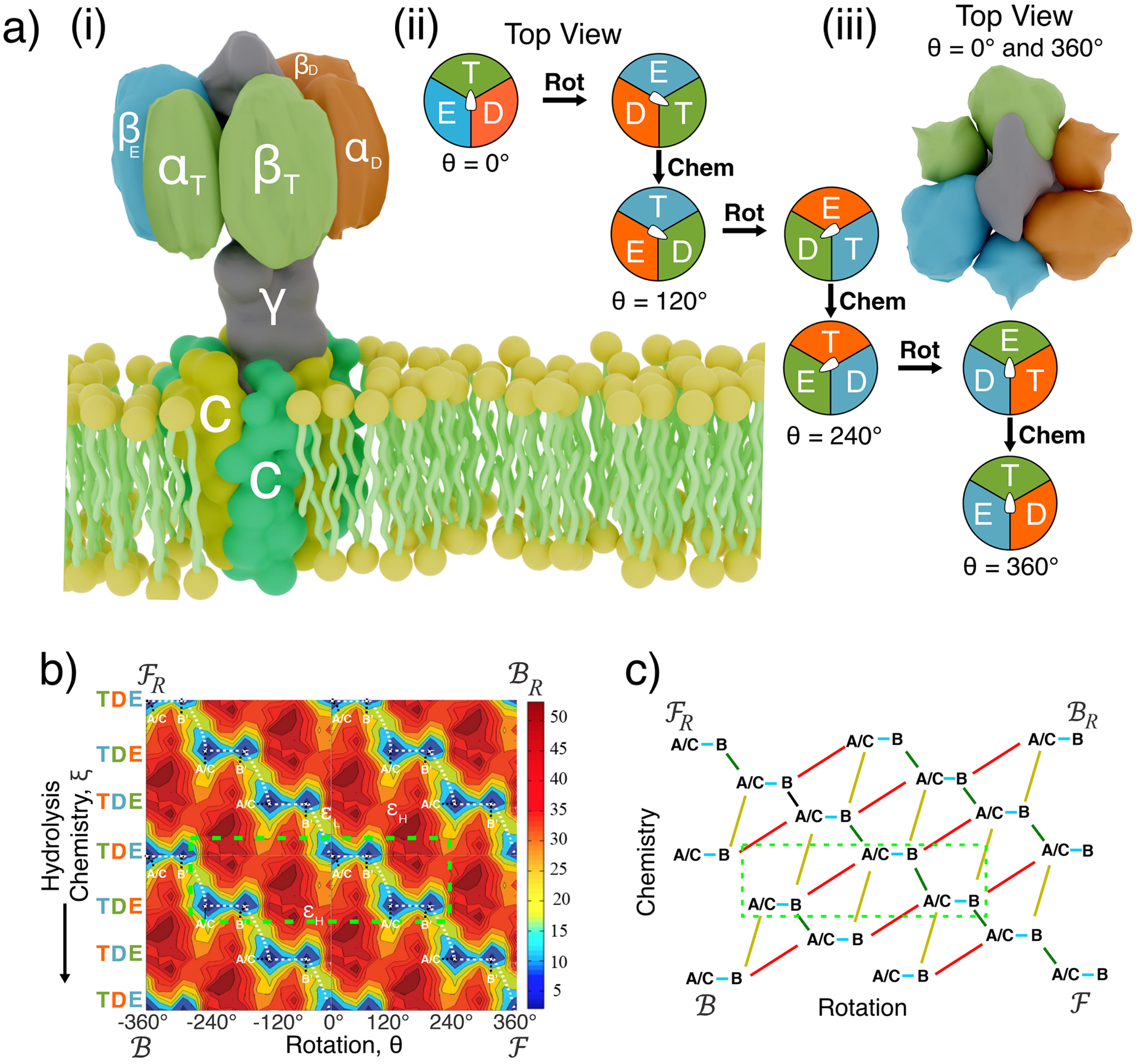

Figure 3. (a) Rotation of the F_1 ATPase coupled to ATP hydrolysis. (i) Graphical representation inspired on the crystal structure of the F_oF_1-ATP synthase. (ii) Top view of the schematic illustration of rotations (horizontal transitions) coupled to chemistry (vertical transitions), where substeps are not shown. The mechanism follows Jencks' rules for vectorial coupling in which chemical and mechanical steps are interleaved. The white letters (T = ATP, D = ADP, E = empty) indicate the chemical states, and the colors (green/orange/blue) of the pie-graphs are used to keep track of the rotational state and are keyed to those in (iii). Top view of the schematic showing the F_1 trimer of dimers and the central γ stalk (gray). (b) A Contour plot of the energy of the F_1 molecule—a trimer of dimers plus a central stalk—computed by energy minimization of the crystal structures subject to having the chemical state of each of the three dimers constrained. The low-energy blue channel running from the upper left (labeled $\mathcal{F}_R$) to lower right (labeled $\mathcal{F}$) defines a priori the most likely trajectory for the F_1 molecule, and the relatively low activation barrier—saddle point—along this channel is labeled ε_L. Paths leading from the upper right-hand corner (labeled $\mathcal{B}_R$) to the lower left-hand corner (labeled $\mathcal{B}$) in contrast must pass over a higher activation barrier labeled ε_H. (c) A kinetic lattice model conveys the same information as the 2D sculpted energy landscape shown to the left. The states (A/C and B) are connected by transitions (red/orange/blue/green) arranged in order of the heights of the activation barriers, from highest (red) to lowest (green). The relative likelihood of the paths $\mathcal{F}/\mathcal{F}_R$ versus $\mathcal{B}/\mathcal{B}_R$ is determined solely by the differences in the activation barriers, while the relative likelihood of the paths $\mathcal{F}$ versus $\mathcal{F}_R$, and the relative likelihood of the paths $\mathcal{B}$ versus $\mathcal{B}_R$, are determined by the free energy released by ATP hydrolysis according to microscopic reversibility.

involving phosphorylation by ATP (T) or dephosphorylation to ATP and the other phosphorylation by ADP + P_i (D·P) or dephosphorylation to ADP + P_i. Trajectory thermodynamics[69] provides the recipe by which these two paths can be averaged, allowing Scheme 2 to be written with effective rate constants as

$$i \underset{\omega_{i,\mathrm{off}}}{\overset{\omega_{i,\mathrm{on}}}{\rightleftharpoons}} i^{\mathrm{P}} \overset{K_{\mathrm{PS}}}{\rightleftharpoons} j^{\mathrm{P}} \underset{\omega_{j,\mathrm{on}}}{\overset{\omega_{j,\mathrm{off}}}{\rightleftharpoons}} j \rightleftharpoons \cdots \rightleftharpoons i.$$

This compaction of notation has led to a widespread error in the literature. The so-called stochastic thermodynamics theory[75] is based on an incorrect approximation known as "local detailed balance", according to which the ratios $\frac{\omega_{i,\mathrm{on}}}{\omega_{i,\mathrm{off}}}$ and $\frac{\omega_{j,\mathrm{on}}}{\omega_{j,\mathrm{off}}}$ are treated as state functions, namely, the exponentials of the "entropy produced in the transitions". This incorrect approximation can even lead some authors to publish results that are patently inconsistent with the second law of thermodynamics, as discussed in ref 37. We must be very clear—away from equilibrium, the ratios of effective state-to-state transition constants are not in general state functions and ineluctably involve a purely kinetic component that depends on the relative activation barriers for binding/release of ATP versus binding/release of ADP + P_i in the states i and j. We must avoid falling into the logical error pointed out by Koenig, Horne, and Mohilner[56] in which theoreticians simply decide which of several thermodynamically allowed processes to ignore. This mistaken "local detailed balance" approximation fails to recognize the importance of the kinetic component. The correct expression for the ratios, shown in eq 1, which was derived and published[69] in 1996, illustrates clearly that the origin of directionality lies in kinetic gating. Indeed, kinetic asymmetry bounds the non-equilibrium behavior of any molecular machine, and the directionality is given by

$$r_0 = \underbrace{\left(\frac{K_i^{\mathrm{T}} K_{\mathrm{PS}} K_{\mathrm{RS}}}{K_j^{\mathrm{T}}}\right)}_{=1} \mathcal{A}_i \mathcal{A}_j^{-1} \tag{2}$$

The ratio of forward (left-to-right) to backward (right-to-left) completions of a cycle in eq 2 is $\mathcal{A}_i \mathcal{A}_j^{-1}$, the intrinsic (load free) directionality of the machine. The directionality in eq 2 does not depend at all on the equilibrium constant for the power-stroke, K_{PS}, or on any other equilibrium constant in the mechanism, or for that matter on any of the free energies of the states. Any thermodynamic advantage of having the transition $i^{\mathrm{P}} \overset{K_{\mathrm{PS}}}{\rightleftharpoons} j^{\mathrm{P}}$ be exergonic is canceled by the requirement of endergonic transitions necessary to reset the system. The idea that the direction of the motion is determined by the free energy released during the conformational change by which a molecular motor moves is simply false. In a recent computational study of Myosin V, Warshel[74] found that the specific conformational change termed the "power-stroke" is in fact endergonic in the normal direction of motion. The widely used terms "force-generating state" or "force-generating transition" have no physical basis and do not make sense. Unlike energy, the storage form of which is potential energy, there is no storage form of force, and hence "force generation" is not a sensible concept. As emphasized by Hill and Eisenberg,[73] the ability to do work against an applied load is a function of an entire cycle and not of any specific state or transition within the cycle. In a recent paper, Hwang and Karplus[42] make the claim that there is a structural basis for distinguishing between "power-stroke" and "Brownian ratchet" mechanisms for molecular motors. These authors arrive at this erroneous conclusion by considering local events in the motor mechanisms, rather than taking on a global perspective of the cycle as a whole. Focusing on a single transition or sequence of transitions is a mistake against which Hill and Eisenberg[73] cautioned in 1981. While there is indeed a structural change by which a motor molecule (Figure 2c) moves, the free energy absorbed from or released to the environment locally plays no role whatsoever in determining the directionality, stopping load, or optimal efficiency of the motor.[72] Hwang and Karplus[42] exacerbated the confusion sown with a cartoon picture in which the effect of ATP is represented by a lightning bolt accompanied by the words "fuel event". Such terminology is extraordinarily misleading—light-driven processes are constrained by the Einstein relations[18] for absorption and emission of light. As we will see in the subsequent discussion on light-driven motors and rotors, the power-stroke can, and often does, determine the directionality of light-driven rotors. All chemical reactions, on the other hand, including phosphorylation of a protein by ATP, are constrained by microscopic reversibility.[19,20] Because of this difference in constraints, no ATP hydrolysis-driven pump or motor can operate by a power-stroke mechanism, even though light-driven motors can and do operate by a power-stroke mechanism.

F_oF_1 ATP Synthase: Diffusion on a Sculpted Energy Landscape. A paradigmatic example of a catalysis-driven biomolecular motor,[76] the F_oF_1 ATP synthase (Figure 3a), is a combination of two motors—the F_1, driven by the catalysis of ATP hydrolysis, and the F_o, driven by protons[77] moving from high to low electrochemical potential across the cellular membrane. When coupled, the dual motor system F_oF_1 is capable of generating ATP, a thermodynamically demanding process that is powered by the energetically downhill transport of protons through F_o. Theoretical studies, based on the solid-state structure of the F_1 motor,[78] have elucidated[77,79] the organizing principle behind the rotary chemical action observed in numerous experiments.[43,61,80,81] These investigations reveal that catalysis-driven biomolecular machines can be understood as systems operating under a simple and universal mechanism—diffusion on a sculpted energy landscape—that applies equally to the pump and motor in Figure 2. An example is shown in Figure 3b taken from the work of Mukherjee and Warshel.[76] The low energy zigzag corridor (shown in blue), running from the upper left-hand to the lower right-hand corner, describes the energetically preferred pathway and is a quintessential manifestation of the zigzag mechanism on a kinetic lattice predicted previously.[68,69] Coupling between rotation and ATP hydrolysis is achieved by kinetic blockage due to the high transition-state energy ε_{H} relative to ε_{L}, the transition-state energy along the favored path. The relative depths of the energy wells—i.e., the free energies of the states—play no role whatsoever in determining directionality. The energy landscape obtained by Mukherjee and Warshel[76] provides a concrete embodiment of coupling by kinetic blockade shown in kinetic lattice models (Figure 3c) of a variety of systems.[68,69,72] The energy surface is sculpted by evolution and reflects the structure−energetics−function paradigm of biological macromolecules. The essential point is that the motion is governed by an energy surface, $U(\vec{r})$, a scalar field with the concomitant identity $\nabla \times \nabla U(\vec{r}) = 0$. Since the system operates at low Reynold's number,[35] the velocity is proportional to the force (gradient of the local potential) that causes the motion.[34] These relations underlie the principle of microscopic reversibility.[19,20] There is no, nor can there be, "curl flux" in a fundamental description of the motion of catalysis driven molecular machines. Similarly, descriptions involving "hopping" from one energy surface to another due to chemical reaction cannot lead to a thermodynamically consistent description of these machines. The very common assertion in the literature that molecular machines are "away-from-equilibrium" is pernicious, not because it is incorrect, but because the statement emphasizes the wrong aspect of molecular machine function. Although the chemical potentials in vivo are such that $\mu_T \gg \mu_D + \mu_P$, the physical motions of the proteins following association/dissociation of ATP (T), ADP (D), and P_i (P) are mechanical equilibrium processes irrespective of the bulk chemical potentials. It is only the relative probabilities of the motions that vary as a function of $\Delta\mu = \mu_T - (\mu_D + \mu_P)$, not the nature of the motion itself. Consider a system with a molecular machine in equilibrium, i.e., with $\Delta\mu = 0$. Every motion accessible to the molecule occurs even in equilibrium, but each trajectory is exactly as likely as its microscopic reverse so there is no net progress in any direction. The F_1-ATPase for which the energy landscape is given in Figure 3b will, at equilibrium, diffuse back and forth predominately but not exclusively in the low energy zigzag channel. There will, of course, be neither net ATP hydrolysis nor synthesis and no net rotation.

When extra ATP is added, the nature of the motions of the atoms that make up the F_1-ATPase molecules do not change. The relative probabilities, however, for those sequences of transitions involving binding ATP and release of ADP + P_i are favored relative to the microscopic reverses of those transitions, in which ADP + P_i bind and ATP is released. In Figure 3b, this bias means that when ATP is in excess, top-to-bottom trajectories are favored relative to bottom-to-top trajectories, a bias which, in combination with the structural zigzag energy landscape, leads to clockwise rotation. The physical motions of the protein do not involve dissipative loss of energy due to friction any more than would those same motions result in frictive energy loss when $\Delta\mu = 0$. The major source of dissipation is futile cycles in which ATP is hydrolyzed without rotation in the desired direction.

Hybrid Artificial-Biological Pumps and Motors. Biomolecular pumps and motors are, as is always the case in nature, complex and exquisitely crafted. The F_1 motor of F_oF_1-ATPase,[5] for example, can use almost 100% of the input chemical energy to drive the motion.[82] These natural machines provide a source of inspiration for those of us who are inclined to tackle the construction of their artificial counterparts. In addition to this incentive, however, they can also be viewed as ready-made devices awaiting adaptation for new tasks, just like oxen waiting for plows. Adaptation of biomolecular motors was initiated by the pioneering work of Kinosita,[83] who was able to mount F_1-ATPase on a surface and attach a fluorescent tag to its rotating subunit, allowing the first direct visualization of the motor's unidirectional rotary motion, a direct confirmation of Boyer's earlier hypothesis.[79,84] Montemagno[85] subsequently adapted and extended attachment chemistries to the task of building a functional "hybrid" molecular machine (Figure 4) based on F_1-ATPase. He attached a long propeller arm to the central γ-subunit ("shaft") of the biological motor and bound its β-subunit to a nanofabricated Ni surface, to create propellers which rotate unidirectionally in response to their fuel, namely ATP.

The programmable nature of DNA binding has made[86] it useful for the creation of a number of hybrid motors, such as bipedal DNA walkers that mimic myosin[87] and other biomolecular walkers. One DNA walker has even been programmed[88] to perform a multistep organic synthesis as it progresses along its track. We point the interested reader to reviews[88,89] that have covered DNA-based and other hybrid motors[90,91] systems extensively. The motor proteins themselves are also beginning to find applications[28,92] outside of the cell as components of complex nanostructures. Examples[93] include the utilization of kinesin in molecular computation arrays as well as, perhaps unsurprisingly, being investigated as a component of synthetic actuators for muscles in prosthetic limbs.

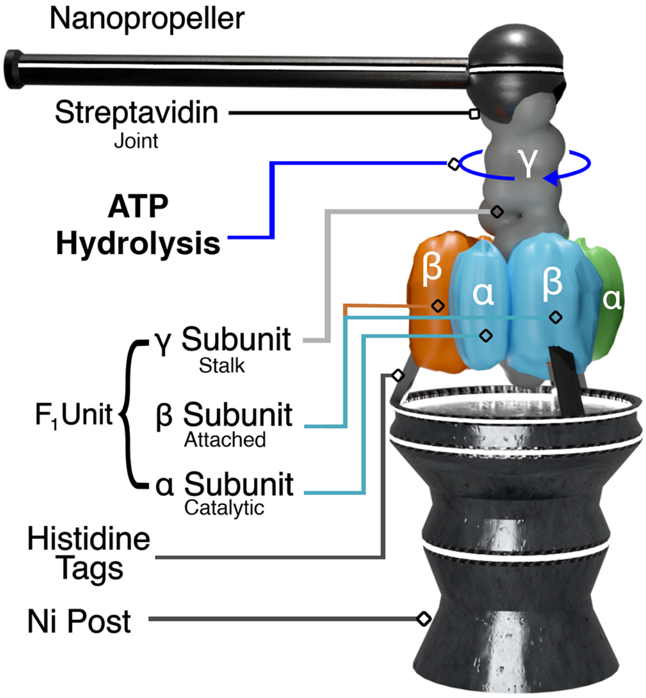

Figure 4. An early hybrid nanopropeller reported by Montemagno using a modified F_1-ATPase motor. The motor was bound to a nanofabricated nickel surface using histidine tags engineered into their β-subunits, while a long synthetic propeller arm was attached to the γ-subunit using biotin/streptavidin linkages. This propeller rotates unidirectionally in response to the addition of ATP to solution and can also be halted by introduction of an inhibitor, NaN_3.

Although the integration of hybrid, or artificial pumps and motors into cells is still in its infancy, progress is being made in this field. As an example, Gale[94] has demonstrated that chloride anionophores, coupled with transmembrane proton gradients, can pump chloride anions selectively inside liposomes in a fueled system that is expected to be generally applicable to many anionophores. Such advances are taking us steadily closer to realizing Hibbs and Feynman's famous prediction[95] that nanomachines may allow us to one day "swallow the surgeon". Non-biological structures may in the fullness of time give rise to a new suite of exploitable properties. We refer the interested reader to a review[96] that covers anion transporters in more depth.

■ LIGHT-DRIVEN ARTIFICIAL MOLECULAR PUMPS AND MOTORS

For a photochemical process $A \rightleftarrows B$, the ratio of the transition constants ω_{AB} and ω_{BA} is given by the Einstein relations,[18] $\frac{\omega_{AB}}{\omega_{BA}} = \frac{\rho(\nu_{BA})}{\frac{8\pi h\nu_{BA}^3}{c^3} + \rho(\nu_{BA})}$, where $\rho(\nu_{BA})$ is the density of photons around the frequency. We can obtain a general relation by taking the illumination source to be a blackbody (bb) radiator at temperature T_{bb}. With the blackbody density-function $\rho(\nu_{AB}) = \frac{8\pi h\nu_{AB}^3}{c^3}[e^{-\Delta G_{AB}/RT_{bb}} - 1]^{-1}$, we find $\frac{\omega_{AB}}{\omega_{BA}} = e^{\Delta G_{AB}/RT_{bb}}$, which can

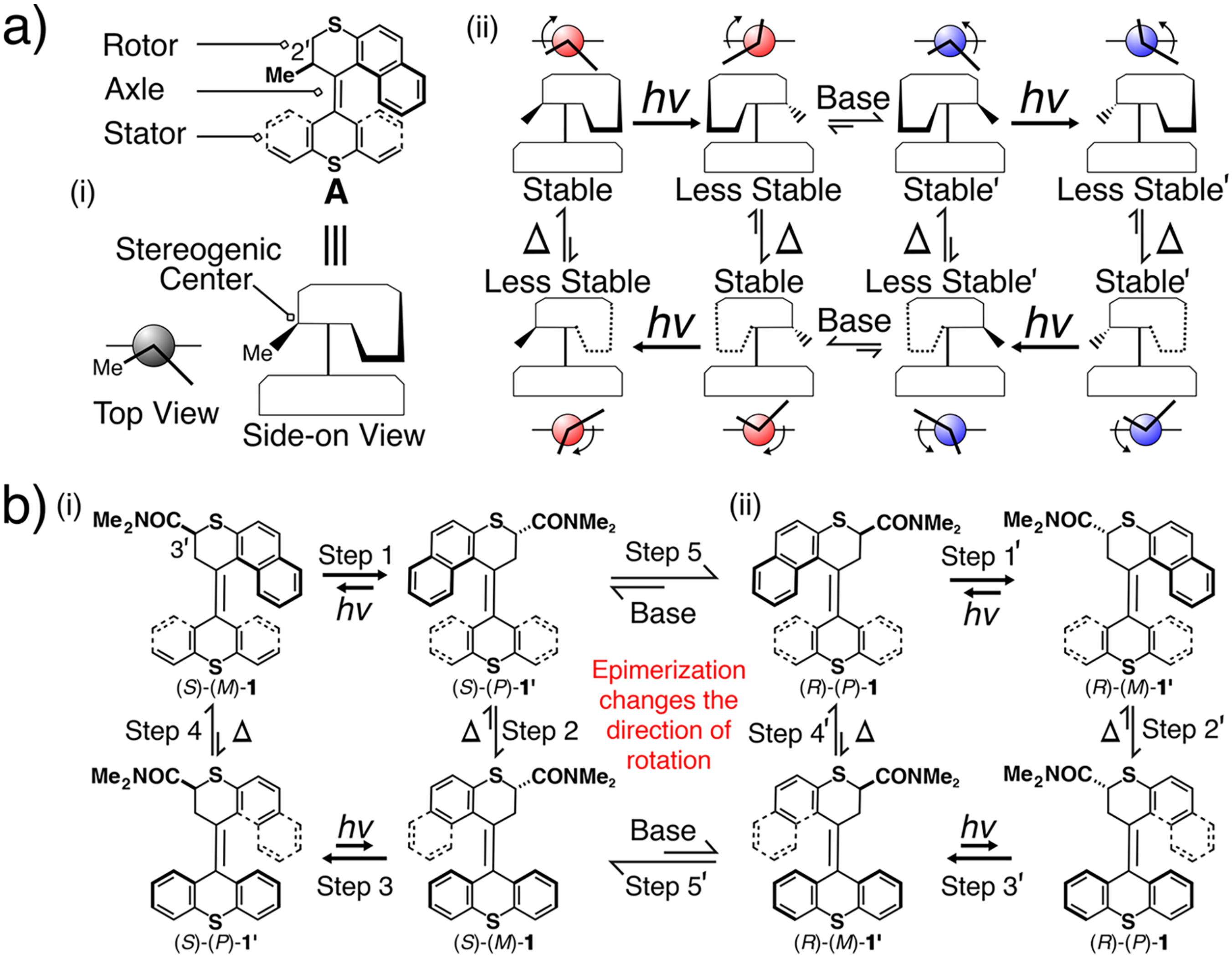

Figure 5. Conceptual and schematic representations of rotary motion in a molecular motor, and the different triggers that control the clockwise and counterclockwise motions. (a) Structural formula of the molecular rotary motor **A**, which comprises a rotor and a stator connected by a C═C double bond (axle) that serves as the axis of rotation. (i) Graphical representations of the top and side-on views of **A** with the stereogenic center carrying a methyl group at C-2′. (ii) Clockwise (left) and counterclockwise (right) rotary cycles. The changes in the orientation of the rotation of the rotor with respect to the stator are indicated by the top and side-on views. The consecutive steps of photoinduced ($h\nu$) isomerization (uphill) and thermal (Δ) helix inversion, repeated a second turn, lead to complete clockwise, or counterclockwise rotation. Base-induced epimerization of the less stable isomers, following photochemical helix inversions, results in reversal of the direction of rotation. (b) The experimental work was carried out on a compound with an electron-withdrawing $CONMe_2$ group at C-3′. Clockwise rotation is initiated by light-induced photochemical isomerization (Step 1) of the stable (*S*)-(*M*)-**1** to give the less stable (*S*)-(*P*)-**1′**, followed by thermal isomerization (Step 2) to afford the stable (*S*)-(*M*)-**1**. Complete clockwise rotation is achieved with consecutive photochemical (Step 3) and thermal (Step 4) isomerizations. The enantiomer can be obtained by based-promoted epimerization (Step 5) of the less stable (*S*)-(*P*)-**1′** to give the stable (*R*)-(*P*)-**1**. Complete counterclockwise rotation (Step 1′→2′→3′→4′) of the stable motor proceeded analogously to the clockwise rotation (Step 1→2→3→4). Base-induced epimerization of the less stable (*R*)-(*M*)-**1′** affords (Step 5′) the stable (*S*)-(*M*)-**1**.

be rewritten in terms of the steady-state ratio between the concentrations as:

$$\left.\frac{[B]}{[A]}\right|_{ss} = e^{\Delta G_{AB}/RT}[e^{-\eta_{Carnot}\Delta G_{AB}/RT}] \tag{3}$$

By use of the expression for the Carnot efficiency in eq 3, $\eta_{Carnot} = \left(1 - \frac{T}{T_{bb}}\right)$. For $T_{bb} \gg T$, $\eta_{Carnot} \to 1$ and the ratio $\left.\frac{[B]}{[A]}\right|_{ss}$ approaches unity—the bright light limit—whereas for $T_{bb} \approx T$, $\eta_{Carnot} \to 0$ and the ratio approaches the standard equilibrium value. The energy storage is maximized under bright light illumination and by choosing a reaction with $G_B \gg G_A$ so that the relaxation upon removal of the illumination source is as large as possible. The transition B→A is the "power-stroke", and in the case of light-driven processes, description of the overall process as operating by a power-stroke mechanism is also appropriate.

Light-Driven Artificial Molecular Motors. In his design of rotary motors, Feringa[7] drew inspiration from the response to light that is the basis for the *cis-trans* isomerization around a carbon−carbon double bond in the retinal chromophore.[97,98] In 2010, Feringa[99] reported the design and synthesis of a molecular motor in which the direction (clockwise, or counterclockwise) of the light-powered rotation can be reversed by base-catalyzed epimerization of the single stereogenic center in the molecular motor. A four-step switching cycle ensures (Figure 5) the unidirectional 360° rotation of the rotor relative to the stator in the molecular motor **A**. The full 360° rotation of one half of **A** relative to the other is driven by two energetically uphill photochemical isomerization steps, each followed by energetically downhill irreversible thermal helix-inversion steps. While the unidirectional rotary motion is governed by the two thermal helix inversion steps, the relative stability of the states and hence the direction of rotation are dictated by the absolute configuration of the stereogenic center. It was hypothesized (Figure 5a) that the direction can be changed from clockwise to counterclockwise by inverting the configuration of the stereogenic center, which can be achieved by the base-catalyzed epimerization of the stereogenic center in the less stable isomer. The epimerization of the motor in a less stable configuration leads to the formation of the thermodynamically more stable isomer. When it came to performing experiments to test this hypothesis, it was necessary to replace the Me group with an electron-withdrawing group (EWG = Me$_2$NOC) in Figure 5b and also to reposition the stereogenic center (2′→3′ position) in the molecular rotor to avoid an undesirable side reaction. Following the photo-induced isomerization of the clockwise rotating form[100] (S)-(M)-**1** to afford the less stable isomer (S)-(P)-**1** with the EWG forced to adopt a sterically unfavorable pseudo-axial orientation, there are two choices. When heated, the motor reverts to the stable (S)-(M)-**1** form by means of a thermal helix-inversion [(P)→(M)]. Under basic conditions, however, the motor undergoes epimerization [(S)→(R)] forming the enantiomer (R)-(P)-**1** which displays counterclockwise rotation on photochemical isomerization, followed by irreversible thermal helix inversion. Overall, the driving force for the reversal in the direction of rotation from clockwise to counterclockwise in the case of this light-driven molecular motor is the relief of strain in the less stable(S)-(P)-**1** when the EWG adopts a more favorable pseudo-equatorial orientation in (R)-(P)-**1**. While this motor operates in a stepwise fashion based on changes in the environment and is hence very slow, other similar motors have been designed by Feringa[101−105] that can operate[106] with power-strokes lasting less than 50 fs (limit of detection), which approaches the theoretical speed limit predicted by quantum mechanics.[107]

Ever since Feringa's seminal paper appeared in *Nature*[108] over 20 years ago, new generations of his light-driven artificial molecular motors (AMMos) keep appearing with constant frequency in the chemical literature[102,103] with added refinements.[109,110] The Groningen group have kept their eyes firmly on applications[111,112] as well as attaching their AMMos to surfaces[113,114] and embedding them in metal−organic frameworks.[115−117] Aside from Feringa's AMMos that are based on the relative rotation of rotors and stators around C═C double bonds, there are promising variants based on C═N double bonds.[118,119] It is clear that there is plenty of room for diversity to visit the design and synthesis of artificial molecular rotary motors.

Light-Driven Artificial Molecular Pump. In 2015, Credi[120] achieved relative unidirectional transport of a crown ether along an asymmetric photoswitchable pseudo-dumbbell (Figure 6) using light and thermal energy. The overall transport of the ring along the pseudo-dumbbell occurs by thermal motion. Directionality is achieved by the photoisomerization of an azobenzene unit, which is intrinsically not bound by microscopic reversibility.[121] The photoswitching controls both the non-covalent interactions (depth of a thermodynamic well) at a recognition site on (E)-**ADB**$^+$ for **DN**[**24**]**C8**, and also the relative transition-state energies (heights of kinetic barriers) for the threading and dethreading over both ends of the pseudo-dumbbell. (E)-**ADB**$^+$ and (Z)-**ADB**$^+$ both comprise a central dialkylammonium recognition site[122] for a dinaphtho[24]crown-8 ether **DN**[**24**]**C8**, a photoswitchable azobenzene unit at one end, and a methylcyclopentyl pseudo-stopper at the other end of the pseudo-dumbbell. As a result of a combination of [N$^+$−H···O] and [C−H···O] hydrogen-bonding interactions between the $-CH_2NH_2^+CH_2-$ unit and the crown ether, and [π···π] stacking interactions between the azobenzene and the naphtho units of the crown ether, the **DN**[**24**]**C8** ring threads onto the pseudo-dumbbell and encircles the dialkylammonium recognition site preferably from the (E)-azobenzene end of (E)-**ADB**$^+$ on account of the relatively small kinetic barrier compared with that imposed by the methylcyclopentyl pseudo-stopper. Irradiation with light triggers the photoisomerization of the azobenzene from its (E)-configuration to its much bulkier (Z)-configuration while curtailing the hydrogen bonding and [π···π] interactions between the ring and (Z)-**ADB**$^+$. These changes in the energy landscape oblige the ring to part company with the pseudo-dumbbell by dethreading over the smaller steric barrier offered by the pseudo-stopper. The reset of the pseudorotaxane is achieved by the conversion, under either irradiation or thermal relaxation, of (Z)-**ADB**$^+$ back to (E)-**ADB**$^+$, and hence the pseudorotaxane can be made to operate continuously and autonomously. This pseudorotaxane can be regarded as a prototypical light-driven artificial molecular pump.

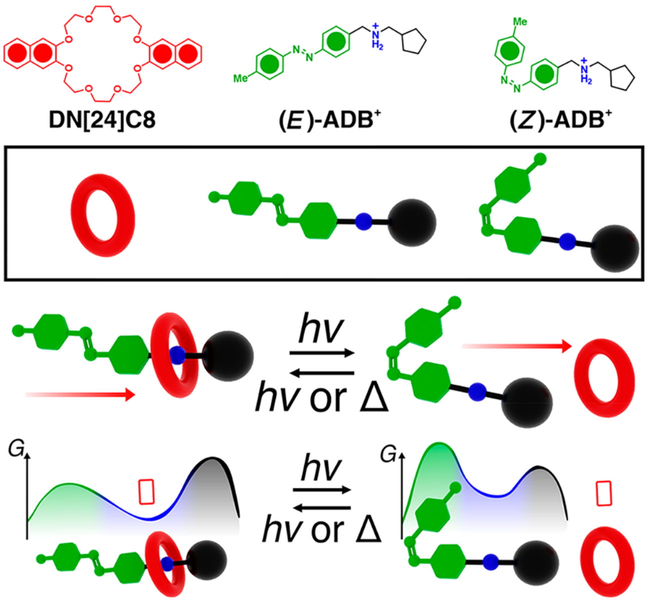

Figure 6. Structural formulas and graphical representations for **DN**[**24**]**C8** and the two configurations of the pseudorotaxane, namely (E)-**ADB**$^+$ and (Z)-**ADB**$^+$. The pseudorotaxane comprises a central dialkylammonium recognition site for the **DN**[**24**]**C8** ring with a photoswitchable azobenzene unit at one end and a methylcyclopentyl pseudo-stopper at the other. The overall transport of the ring along the pseudo-dumbbell occurs by thermal motion. Directionality is imparted by the light-induced (E)- → (Z)-**ADB**$^+$ transition which is intrinsically not bound by microscopic reversibility. The energy profiles represent the free energy of the pseudorotaxane as a function of the position of the ring along the pseudo-dumbbell.

Credi has reviewed the latest research from the Bologna group on photoactive artificial molecular machines (AMMs) in

Chemical Communications,[123] *Advanced Materials*,[124] and *Chemical Reviews*.[125] It is worthy of note that similar effects can be achieved by the electrical driving of a small molecular rotor.[126]

ARTIFICIAL MOLECULAR PUMPS BASED ON ENERGY RATCHETS

The theoretical basis for understanding free-energy transduction is found in the work of Onsager,[33] who derived the reciprocal relations for which he was awarded the Nobel Prize in Chemistry[127] in 1968. Onsager's work had already set the stage for the development of chemical relaxation techniques used to study the kinetics of very fast chemical reactions, research that had been awarded the Nobel Prize in Chemistry[128] to Norrish,[129] Porter,[130] and Eigen[131] the previous year. Norrish and Porter were recognized for their use of light to disturb chemical equilibria. Eigen was recognized for the development of techniques by which rapid changes in thermodynamic parameters, e.g., electric field, pressure, or temperature, could be driven. He also developed the theory by which the resulting changes in chemical concentrations could be interpreted in terms of the kinetics of the chemically reacting system. Unfortunately, the Nobel citation,

> *for their studies of extremely fast chemical reactions, effected by disturbing the equilibrium by means of very short pulses of energy...*

which implies that a pulse of light energy is more or less the same as energy introduced by a rapid change in thermodynamic parameters, is misleading. The constraints on how light works to pump a chemical system to a non-equilibrium state—quantified by the Einstein relations[18]—are very different from those arising from microscopic reversibility[19,20] which constrains how thermodynamic perturbations influence a chemical reaction. The essential feature necessary for energy transduction from a time-dependent thermodynamic perturbation is a molecular structure that provides an energy well flanked by two energy barriers, where the well and at least one of the barriers are influenced by the perturbation. The paradigmatic model is a Michaelis–Menten[71] mechanism with time-dependent rate constants.[132] For any constant environment the ratio between the concentrations of the product (P) and substrate (S) of the catalyzed reaction is the same equilibrium constant, $\left.\frac{[\mathrm{P}]}{[\mathrm{S}]}\right|_{\mathrm{eq}} = K_{\mathrm{eq}}$, that pertains in the absence of the catalyst. In the presence of external time-dependent driving, however, energy can be absorbed by the enzyme and transduced to maintain a non-equilibrium steady state between the product and the substrate, $\left.\frac{[\mathrm{P}]}{[\mathrm{S}]}\right|_{\mathrm{ss}} = K_{\mathrm{eq}}\langle \mathrm{e}^{\mathcal{W}_{\mathrm{pd},\mathcal{S}}/RT}\rangle$, where $\langle \mathrm{e}^{\mathcal{W}_{\mathrm{pd},\mathcal{S}}/RT}\rangle$ is the exponential average of the path-dependent (pd) energy absorbed by the catalyst from external perturbations. The weighted average is over all possible paths $\mathcal{S}$, leading from substrate to product.[132] and the kinetic weights are the probabilities $\pi_{\mathcal{S}}$ for a specific trajectory $\mathcal{S}$. These weights obey microscopic reversibility,[19,20] $\frac{\pi_{\mathcal{S}}}{\pi_{\mathcal{S}^\dagger}} = K_{\mathrm{eq}}\,\mathrm{e}^{\mathcal{W}_{\mathrm{pd},\mathcal{S}}/RT}$, for every $\mathcal{S}$, a general organizing principle for molecular machines, where $\mathcal{S}^\dagger$ is the microscopic reverse of $\mathcal{S}$. The importance of the individual trajectories in assessing the possibilities of free-energy transduction has led to the development of the field of trajectory thermodynamics,[133] which has as its intellectual underpinnings the Onsager–Machlup thermodynamic-action theory[34] and which is based on the very solid principle of microscopic reversibility.[19,20] The only "near-equilibrium" requirement for application of this theory is that the system be near mechanical equilibrium such that the physical velocities are proportional to the forces that cause them — the low Reynolds number[35] regime — that applies to all molecular machines in solution. Trajectory thermodynamics holds arbitrarily far from thermodynamic equilibrium, i.e., the chemical potentials of the various components and molecular fuels of the system can be very different from one another.

Redox-Driven Artificial Molecular Pumps (AMPs) Based on Rotaxanes. In 2013, we synthesized[134] a constitutionally asymmetric pseudo-dumbbell, **PDB**$^+$, designed (Figure 7) to generate relative unidirectional motion in which a cyclobis(paraquat-*p*-phenylene) (**CBPQT**$^{4+}$) ring threads at one end of the pseudo-dumbbell and dethreads over the other end. This pseudo-dumbbell **PDB**$^+$ consists (Figure 7) of a neutral 2-isopropylphenyl (2IPP) group, providing a steric barrier at one end, an electron-rich 1,5-dioxynaphthalene (DNP) unit in the middle of an oligo(ethylene glycol) chain and a positively charged 3,5-dimethylpyridinium (PY$^+$) group, providing an electrostatic barrier at the other end. The

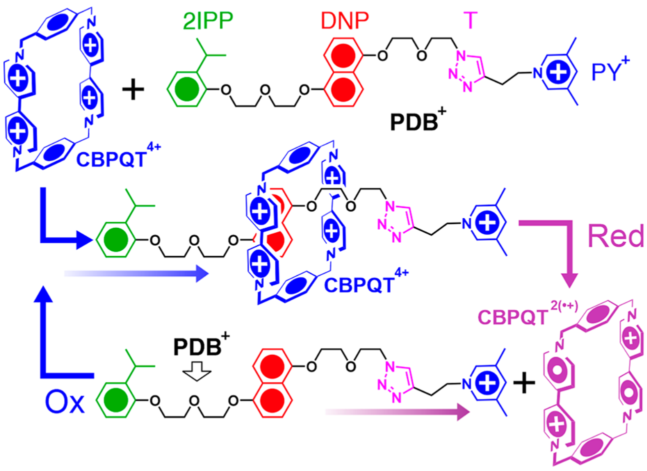

Figure 7. Structural formulas for the **CBPQT**$^{4+}$ and **CBPQT**$^{2(\bullet+)}$ rings, as well as the **PDB**$^+$ pseudo-dumbbell. **PDB**$^+$ consists of a centrally located electron-rich 1,5-dioxynaphthalene (DNP) recognition site (red) for the electron-deficient **CBPQT**$^{4+}$ ring (blue), a neutral 2-isopropylphenyl (2IPP) unit (green) at one end and a positively charged 3,5-dimethylpyridinium (PY$^+$) unit (blue) at the other end, linked with a triazole (T) ring (magenta). The PF_6^- counterions are omitted for the sake of clarity. Unidirectional threading of the **CBPQT**$^{4+}$ ring and dethreading of the **CBPQT**$^{2(\bullet+)}$ ring along **PDB**$^+$ are realized by altering the redox states of the ring. Under oxidative conditions, the **CBPQT**$^{4+}$ ring binds to the DNP unit following passage over the neutral 2IPP unit rather than over the positively charged PY$^+$ unit on account of Coulombic repulsion. Reduction of **CBPQT**$^{4+}$ to **CBPQT**$^{2(\bullet+)}$ switches off the donor–acceptor interactions with the DNP unit and attenuates the Coulombic repulsion between the ring and the PY$^+$ unit, allowing the ring to leave the **PDB**$^+$ over the PY$^+$ unit and re-enter bulk solution. Upon oxidation, the ring reverts to its tetracationic state, namely **CBPQT**$^{4+}$, restarting the redox cycle and demonstrating the pseudo-dumbbell's repeatable behavior as an energy ratchet.

electron-rich DNP unit has good binding affinity for the electron-deficient **CBPQT**$^{4+}$ ring in its oxidized state by virtue of donor−acceptor interactions. Reduction of the ring negates these interactions, resulting in a lower binding affinity for the reduced **CBPQT**$^{2(\bullet+)}$ form. Hence, when fully oxidized, the **CBPQT**$^{4+}$ ring threads onto the dumbbell and binds to the DNP recognition site, forming a [2]pseudorotaxane. Threading occurs predominantly over the neutral 2IPP group on account of the strong Coulombic repulsion between the tetracationic cyclophane and the PY^{+} group. When a reductant is added, the **CBPQT**$^{4+}$ ring is reduced to **CBPQT**$^{2(\bullet+)}$, switching off the donor−acceptor interactions with the DNP recognition site. Dethreading occurs primarily over the PY^{+} group as a result of the significantly decreased Coulombic repulsion, thus completing a cycle of unidirectional threading and dethreading. This redox-driven unidirectional motion can also be powered autonomously by visible-light (λ = 450 nm) energy in the presence of a photosensitizer, namely Ru(bpy)$_3^{3+}$, and a sacrificial electron donor, namely phenothiazine. This AMP prototype operates by a flashing energy ratchet mechanism: the structural arrangement of a steric barrier, a recognition site, and an electrostatic barrier forms what we now propose to call a pumping cassette—a principal active component of non-equilibrium molecular machines.

The demonstration of unidirectional motion[120,123] in intelligently designed rotaxanes and catenanes has fostered a new age of synthetic non-equilibrium[37,135] chemistry. These mechanically interlocked molecules[9] (MIMs) lend themselves to the incorporation of fleets of components which are capable of working in an integrated fashion, harnessing external energy for the assembly of highly non-equilibrium systems, demonstrating pump-like and motor-like activity. Let us begin by considering artificial molecular pumps (AMPs). While early implementation[120] used donor−acceptor recognition sites as switchable components in prototypes of AMPs, they were limited in the amount of energy that could be captured and utilized to drive non-equilibrium processes. A radically new approach[136] that offers the opportunity of transducing much greater amounts of energy became possible as a result of the discovery in 2010 by Trabolsi[137] of the formation of a very strong 1:1 trisradical tricationic complex between CBPQT$^{2(\bullet+)}$ and BIPY$^{\bullet+}$ units.[138] This discovery led to the design and synthesis of several AMPs containing radically driven pumping cassettes.

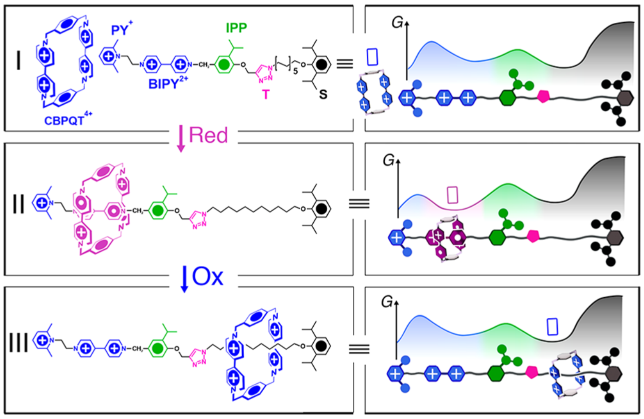

Figure 8. Structural formulas (left) and graphical representations, overlaying energy landscapes (right) for one redox cycle of the Mark II artificial molecular pump (AMP). The dumbbell (**DB**$^{3+}$) consists of a positively charged 2,6-dimethylpyridinium (PY^{+}) Coulombic barrier (blue), a redox-switchable bipyridinium (BIPY^{2+}) recognition site (blue), an isopropylphenylene (IPP) steric barrier (green), and a triazole (T) ring (magenta), linking the pumping cassette to an oligomethylene collecting chain, terminated by a (black) 2,6-diisopropylphenyl stopper (S). In stage I, the positively charged **CBPQT**$^{4+}$ ring in bulk solution (MeCN) is prevented from threading onto the dumbbell because of the electrostatic barrier presented by the PY^{+} unit and the steric barrier provided by the S stopper. In stage II, when all the BIPY^{2+} units on the ring and in the dumbbell have been reduced chemically (Zn dust) to **CBPQT**$^{2(\bullet+)}$ and BIPY$^{\bullet+}$, it becomes possible, because of decreased Coulombic repulsion, for the ring to pass over the PY^{+} unit and form a trisradical tricationic complex (purple) with the BIPY$^{\bullet+}$ unit in the dumbbell. In stage III, the pumping cassette is switched by chemical (NOPF$_6$) oxidation, removing the radical stabilization. The now strong Coulombic repulsion between the **CBPQT**$^{4+}$ ring and the BIPY^{2+} and PY^{+} units in the dumbbell enforces ring traversal over the IPP steric barrier and onto the collecting chain by thermal activation at room temperature, thus forming a [2]rotaxane in an away-from-equilibrium metastable state.

Redox-driven unidirectional translation along a dumbbell, which carries a collecting chain terminated by a stopper at one end and a pumping cassette at the other end, provided[120] the basis for the synthesis of two generations of AMPs—namely Mark I[139] and Mark II[140] artificial molecular pumps. The dumbbell (**DB**$^{3+}$) employed (Figure 8) in the Mark II AMP consists of (i) a cationic 2,6-dimethylpyridinium (PY^{+}) Coulombic barrier attached to (ii) a redox-switchable bipyridinium (BIPY^{2+}) unit[138] with (iii) an isopropylphenylene (IPP) steric barrier linked through (iv) a triazole (T) unit to (v) an oligomethylene collecting chain terminated by (vi) a sterically bulky 2,6-diisopropylphenyl stopper (S). The three components (i), (ii), and (iii) constitute the radically driven pumping cassette.[141] In stage I, the **CBPQT**$^{4+}$ ring is reduced chemically to **CBPQT**$^{2(\bullet+)}$ which can pass over the PY^{+} Coulombic barrier to form a trisradical tricationic complex with the reduced BIPY$^{\bullet+}$ unit. In stage II, the strong Coulombic repulsion between the **CBPQT**$^{4+}$ ring and the BIPY^{2+} unit in the pumping cassette, which arises as a result of oxidation, causes the formation of a metastable state in which the ring is located up against the IPP steric barrier. In stage III, the ring ultimately passes over the barrier by thermal activation to become kinetically trapped on the oligomethylene collecting chain, forming a [2]rotaxane. This kinetically stable, away-from-equilibrium [2]rotaxane can subsequently recruit a second **CBPQT**$^{4+}$ ring from solution by undergoing the same redox cycle again, to form a [3]rotaxane. It should be noted that the IPP steric barrier traps the first ring on the collecting chain, preventing return to the BIPY$^{\bullet+}$ recognition site during recruitment of the second ring during a subsequent redox cycle. The steric and Coulombic barriers have been optimized[136] such that (i) a **CBPQT**$^{2(\bullet+)}$ ring in solution can thread onto the dumbbell to bind with the BIPY$^{\bullet+}$ recognition site in its reduced state, (ii) the steric barrier is not so great that it prevents the passage of the **CBPQT**$^{4+}$ ring, driven by Coulombic repulsion from the BIPY^{2+} unit in its oxidized state, and (iii) when the bipyridinium unit is reduced in subsequent redox cycles, passage of a ring from the bulk over the electrostatic barrier is energetically more favorable than the ring on the collecting chain passing back over the steric barrier, making it possible to collect two rings sequentially. Importantly, the first ring on the collecting chain has no measurable effect when recruiting the second ring. In summary, we have focused on the second version of an

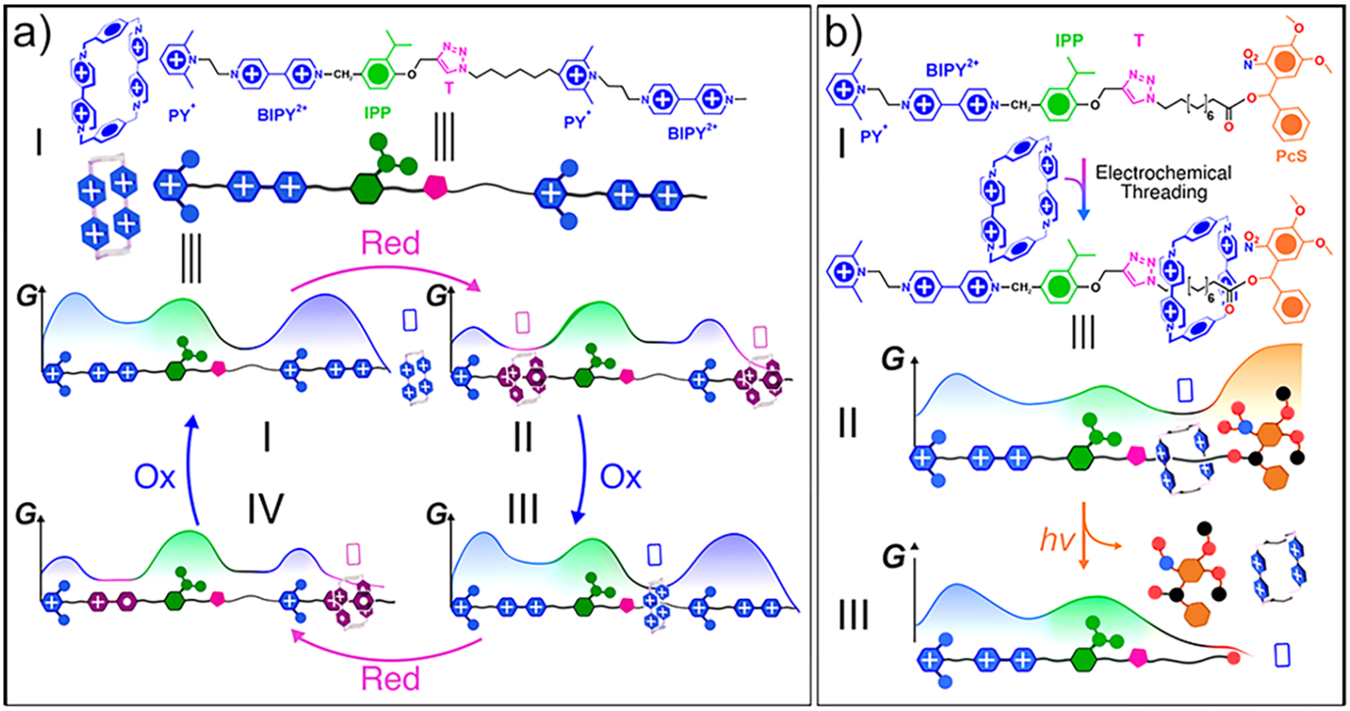

Figure 9. Structural formulas of dumbbells and graphical representations overlying energy profiles for a molecular dual pump (MDP) and a photoswitchable molecular pump (PcMP). (a) The molecular dual pump (MDP) comprises two Mark II pumping cassettes linked together in a head-to-tail manner. The four stages (I→II→III→IV→I) occur over two redox cycles. Stage I→II involves the **CBPQT**$^{4+}$ rings in bulk solution being reduced along with both BIPY^{2+} units in the dumbbell. A **CBPQT**$^{2(\bullet+)}$ ring passes over the terminal PY^{+} onto the BIPY$^{\bullet+}$ unit forming a trisradical tricationic complex. Another **CBPQT**$^{2(\bullet+)}$ ring binds onto the terminal BIPY$^{\bullet+}$ unit at the other end of the dumbbell. Upon oxidation (stage II→III) the **CBPQT**$^{4+}$ ring on the end of the dumbbell dissociates rapidly back to bulk without participating in the overall unidirectional motion. The critical **CBPQT**$^{4+}$ ring, located between the PY^{+} and IPP barriers, is forced by Coulombic repulsion to overcome the IPP steric barrier forming a stable (and isolable) [2]rotaxane. In stage III→IV, reduction of the [2]rotaxane results in the formation of the **CBPQT**$^{2(\bullet+)}$ ring which passes over the centrally located PY^{+} unit, forming a trisradical tricationic complex, i.e., a [2]pseudorotaxane. Upon oxidation in stage IV→I, the [2]pseudorotaxane dissociates and releases the **CBPQT**$^{4+}$ ring back into the bulk solution. In summary, the MDP is capable of transporting a **CBPQT**$^{4+}$ ring from solution unidirectionally along its dumbbell component and back into solution. (b) The photoswitchable molecular pump (PcMP) comprises a Mark II pumping cassette linked by a triazole (T) ring (magenta) to an oligomethylene collecting chain which is terminated by a photocleavable stopper (PcS, orange). In stage I→II, a redox cycle forms a metastable [2]rotaxane. In stage II→III, irradiation with UV (λ = 365 nm) light results in cleavage of the PcS stopper, breaking the mechanical bond, to release the **CBPQT**$^{4+}$ ring into bulk solution.

AMP[140] that is able to move a couple of rings unidirectionally under redox control and store them on a collecting chain in a non-equilibrium state.

Controlling Ring Capture and Release. Unlike molecular motors, the molecular pumps that we have described reach a non-equilibrium steady state when the collecting chains of the final [*n*]rotaxanes are saturated with rings. In order to recover the initial dumbbell, it is desirable to release the captured ring(s) in a controlled manner.

Two AMPs (Figure 9) that allow controlled capture and release have been described recently in the literature.[142,143] Both of these AMPs have cassettes based on the Mark II pump[140] (Figure 8) and form kinetically stable rotaxanes with a **CBPQT**$^{4+}$ ring following either a chemical or an electrochemical redox cycle. In the molecular dual pump[142] (MDP), a partial pumping cassette consisting (Figure 9a) of 2,6-dimethylpyridinium (PY^{+}) and bipyridinium (BIPY^{2+}) units is connected to the collecting chain of the first pump in a head-to-tail fashion. After a single redox cycle (I→II→III), a [2]rotaxane is formed (~85% reliability) because dethreading of the **CBPQT**$^{4+}$ ring is prevented by the PY^{+} Coulombic barrier in the middle of the dumbbell. Under reducing conditions (III→IV), the BIPY^{2+} units are converted into the radical cationic BIPY$^{\bullet+}$, attenuating the Coulombic repulsion with the **CBPQT**$^{2(\bullet+)}$ ring and re-introducing the possibility for radical−radical complexation. The IPP steric barrier prevents the collected ring from taking a retrograde step, resulting in its forward movement to the terminal BIPY$^{\bullet+}$ recognition site. Subsequent oxidation ejects (IV→I) the ring from the MDP, having transferred it unidirectionally across its length.

In the photocleavable molecular pump[143] (PcMP), the steric stopper of the Mark II pump[140] (Figure 8) is replaced (Figure 9b) by an *o*-nitrobenzyl alcohol derivative[144] as a photocleavable stopper (PcS). The PcS can detach from the collecting chain as a *o*-nitrosobenzaldehyde under light irradiation. A **CBPQT**$^{4+}$ ring from solution can be threaded on the dumbbell with a similar mechanism of the Mark II pump as the energy barrier of the PcS is redox independent. Upon UV (λ = 365 nm) irradiation (II→III), the PcS is cleaved from the dumbbell, resulting in the release of the ring.

The intermediate [2]rotaxanes formed by either (i) MDPs or (ii) PcMPs can be isolated from free **CBPQT**$^{4+}$ solution without causing dethreading of their captured rings. The release of the ring is controlled by the use of (i) a chemical or an electrochemical redox cycle or (ii) continuous UV irradiation. Thus, by utilizing MDPs or PcMPs, not only can **CBPQT**$^{4+}$ rings be moved along the dumbbells unidirection-

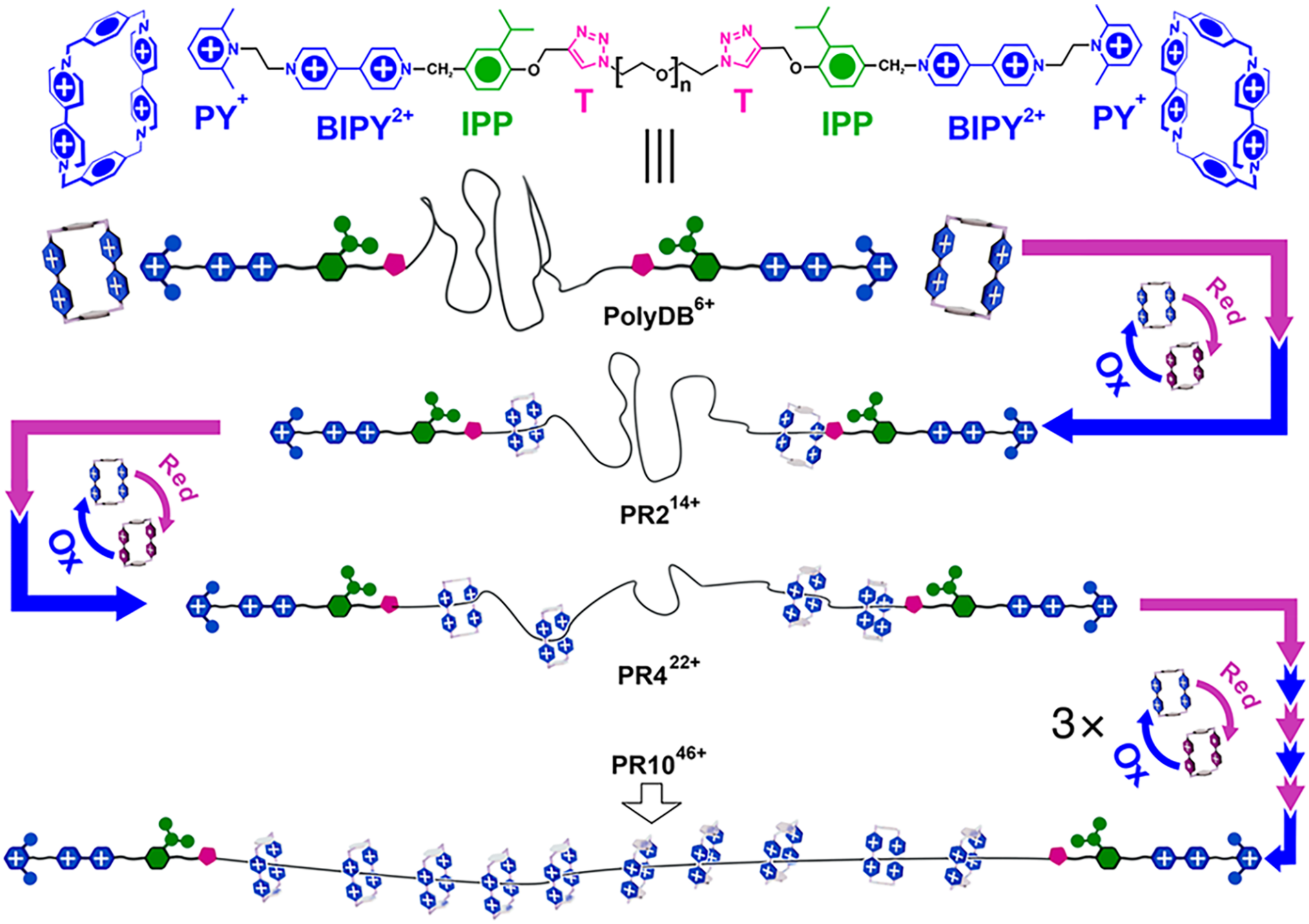

Figure 10. Structural formulas of the starting polydumbbell (**PolyDB**$^{6+}$) and the **CBPQT**$^{4+}$ rings employed in the precise synthesis of an arithmetic series of polyrotaxanes (**PR2**$^{14+}$, **PR4**$^{22+}$, ..., **PR10**$^{46+}$), which is illustrated graphically starting from **PolyDB**$^{6+}$, employing a molecular duet pump with two pumping cassettes, acting in unison under redox control, feeding on two rings simultaneously, one from each end of the polydumbbell component. **PolyDB**$^{6+}$ consists of pairs of positively charged 2,6-dimethylpyridinium (PY$^+$) Coulombic barriers (blue), redox-switchable bipyridinium (BIPY^{2+}) units (blue), isopropylphenylene (IPP) steric barriers (green), and triazole (T) rings (magenta) all joined to a poly(ethylene glycol) (PEG) chain (M_n = 2000 g mol^{-1}) where *n* represents approximately 50 repeating units. The pumping cassettes in the duet pump are operated by either chemical or electrochemical redox cycles. At the outset of the syntheses **PolyDB**$^{6+}$ repels the 8-fold molar excess of **CBPQT**$^{4+}$ rings in solution (MeCN) as a result of strong Coulombic repulsions with the PY$^+$ termini. When a chemical reductant (CoCp$_2$) is added or a negative potential (− 700 mV) is applied, both the rings and dumbbell are reduced, allowing two **CBPQT**$^{2(\bullet+)}$ rings to thread onto the BIPY$^{\bullet+}$ recognition sites at each end of the dumbbell, forming two trisradical tricationic complexes (purple). On addition of a chemical oxidant (NOPF$_6$) or application of a positive potential (+ 1400 mV), the **CBPQT**$^{4+}$ rings thread over the IPP steric barriers onto the PEG chain as a result of the strong Coulombic repulsions from BIPY^{2+} and PY$^+$ units to afford **PR2**$^{14+}$. Repetition of the redox cycle produces **PR4**$^{22+}$, **PR6**$^{30+}$, **PR8**$^{38+}$, and **PR10**$^{46+}$ precisely according to the number of redox cycles. With each subsequent cycle, the polyrotaxane product is driven further and further from equilibrium.

ally, but we are also granted access to a cargo-release platform that can be accomplished in a controlled way. This newfound control suggests the possibility of using AMPs to generate concentration gradients across artificial membranes.[94,145,146]

Polyrotaxane Synthesizer. A polyrotaxane synthesizer (Figure 10) has been reported[147] which, using a pair of pumping cassettes, progressively builds up main chain poly[*n*]rotaxanes, where *n* follows an odd, arithmetic series, with an even number, ($n - 1$), of rings, through repeated redox cycles. This synthesizer demonstrates the synthetic utility of AMPs. The polymer dumbbell (**PolyDB**$^{6+}$) of this AMP incorporates two inward-facing Mark II cassettes as the termini of a poly(ethylene glycol) (PEG) (M_n = 2000) collecting chain. Using chemical or electrochemical redox cycles in one pot, this duet pump[148,149] is able to load two rings simultaneously per cycle from the solution. [3]/[5]/[7]/[9]/[11]Rotaxanes which form with 2/4/6/8/10 rings can be synthesized selectively by controlling the number of redox cycles. These polyrotaxanes have $14^+/22^+/30^+/38^+/46^+$ positive charges on the **PolyDB**$^{6+}$. The PEG chain, initially in a random coil conformation, becomes increasingly stretched and rigid as more tetracationic rings are pumped onto it, as shown[147] by DOSY NMR spectroscopy. The Coulombic energy of the poly[*n*]rotaxanes (n = 3, 5, 7, 9, 11) increases with each redox cycle, roughly proportional to $(n - 1)^2$, and hence the polymer is driven further and further away-from-equilibrium. This increase in Coulombic energy brings us to a very important point. Similar processes in other contexts are often termed[150−154] "dissipative assembly", but this term is misleading. Dissipation certainly accompanies the repetitive oxidation and reduction cycles that provide the energy for pumping, but the key feature allowing operation of the polyrotaxane synthesizer is kinetic asymmetry arising from the specific arrangement of the pumping cassette, and in particular of the PY^+ and IPP units that provide the kinetic barriers. If the kinetic asymmetry would be inverted by exchanging the positions of the PY^+ and IPP units on each pumping cassette, the dissipation due to externally enforcing redox cycling would not decrease, but there would be no pumping. Kinetic asymmetry guided redox-driven creation of high energy mechanically interlocked polymers, in which the rings demonstrate very little affinity for the collecting chain, would have been impossible by any conventional synthetic approach. The generation of this homologous series of polymers by a molecular duet pump demonstrates the promise of AMPs, not only for the control of energy, through their ability to store cargo away from equilibrium, but also for allowing us to reach into hitherto inaccessible areas of molecular space, creating highly unnatural organic entities with unexplored properties.

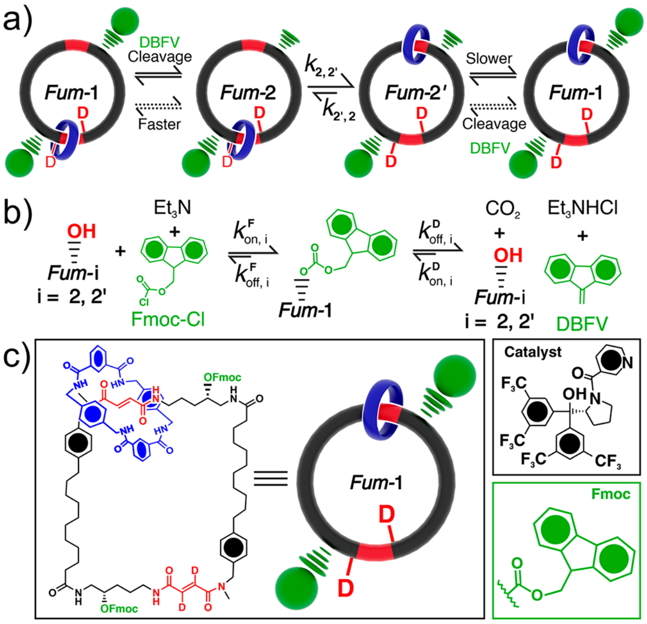

Figure 11. A catalysis-driven synthetic molecular motor. (a) The kinetic mechanism for the interconversion between ***Fum*-1**, ***Fum*-2**, and ***Fum*-2′**. (b) The mechanism of the overall conversion of Fmoc-Cl to DBFV and carbon dioxide (CO_2) at the two hydroxyl groups on the loop. The relative length of the arrows indicates in which direction the equilibrium is shifted. (c) Graphical representation and structural representation of the large loop and the catalyst.

■ ARTIFICIAL MOLECULAR MOTORS BASED ON INFORMATION RATCHETS

The Mark I and Mark II AMPs are based on a flashing energy ratchet mechanism where modulation of energy by redox of $CBPQT^{4+/2(\bullet+)}$ rings and $BIPY^{2+/\bullet+}$ units is an essential requirement for pumping. Catalysis-driven pumps, e.g., ion pumps, ATP-driven motors (Figure 2), and F_1-ATPase (Figure 3), do not and cannot work by a flashing energy ratchet mechanism. The essential requirement is a feedback mechanism by which the reactivity (lability) of the substrate (S, e.g., ATP) and product (P, e.g., ADP + P_i) is determined by the mechanical state of the pump or motor. If in one state the motor is specific for substrate and in another the motor is specific for product, a chemical potential difference $\mu_S - \mu_P > 0$ drives the motor through its kinetic cycle from the S-specific state to the P-specific state, irrespective of the free energies of any of the states.

A Catalysis-Driven Molecular Motor. In 2016, Leigh[155] reported the first example (Figure 11) of a catalysis-driven synthetic molecular motor based on a [2]catenane which operates by using an information ratchet. The catenane has two fumaramide[156] (*Fum*) recognition sites, positioned on opposite sides of a large loop, that interact with a much smaller benzylic amide ring. Directional circumrotation (Figure 11a) by the small ring round the large loop between the two recognition sites is controlled by the addition and removal (Figure 11b) of bulky protecting groups. These groups are introduced onto the hydroxyl groups by catalytic esterification with fluoromethoxycarbonyl chloride (Fmoc-Cl). Note that the catalyst, shown in Figure 11c, is bulky, and hence the esterification is sterically hindered when the small blue ring is close to the hydroxyl group. Removal of the protecting groups occurs spontaneously by non-catalytic cleavage in the presence of triethylamine (Et_3N) to give dibenzofulvene (DBFV) and carbon dioxide (CO_2). Because the cleavage proceeds non-catalytically, the rate is insensitive to whether the small blue ring is close to or far from the protecting group that is being cleaved. There are three co-conformers of the [2]catenane, differing in the location of the small blue ring in relation to the protecting groups on the loop. In one of the co-conformers, ***Fum*-1**, both of the hydroxyl groups on the loop are esterified with Fmoc-Cl. While in co-conformer ***Fum*-2**, the small blue ring is situated close an Fmoc protecting group, in co-conformer ***Fum*-2′**, the small blue ring is located far away from the Fmoc protecting group. The concentration of reagents was controlled so that, at any one time, only one hydroxy group at most was de-esterified. The result of adding and removing a protecting group is that Fmoc-Cl is converted into DBFV, releasing about 25*RT* of energy, an amount roughly equal to the energy released by ATP hydrolysis. The ***Fum*-2** ⇌ ***Fum*-2′** equilibrium is shifted to the right by the steric repulsion between the small blue ring and the Fmoc protecting group. Thus, the conversion is one that many would term a "power-stroke". The direction of the equilibrium shift at first sight suggests that the small blue ring undergoes clockwise circumrotation, around the loop in the order ***Fum*-1→*Fum*-2→*Fum*-2′→*Fum*-1**. The catalytic esterification, however, with Fmoc-Cl is faster for ***Fum*-2→*Fum*-1** than it is for ***Fum*-2′→*Fum*-1**. This kinetic effect argues, instead, in favor of a counterclockwise circumrotation of the small blue ring round the loop in the order ***Fum*-1→*Fum*-2′→*Fum*-2→*Fum*-1**. When a quantitative analysis was performed under the constraints of microscopic reversibility,[19,20] the latter conclusion was vindicated − an order also observed experimentally.[155] It must be emphasized that the mechanism of operation of catalysis-driven motors is very different from that for pumps and motors driven by external modulation. In the case of the latter, the energy of binding of a recognition site is changed as a function of external modulation, whereas in the case of the former, the key factor is gating catalysis by allosteric interactions, and the modulation of the binding energy of recognition sites is unimportant. Catalysis-driven synthetic molecular motors operate using an information ratchet mechanism.

The prototype for this catalysis-driven artificial molecular motor (AMMo) can be traced back to a molecular information ratchet which was described by Leigh[157] in 2007. Aside from the information ratchet, catenane-based AMMos, which operate by energy ratchet mechanisms, have also been described by Leigh.[158−160] In 2003, it was shown[158] for the first time that unidirectional motion can be induced in a [3]catenane in which the two smaller rings interfere with each other's transitions between recognition sites on the larger ring, ensuring stimuli-driven unidirectionality of the two smaller rings around the larger ring. We can expect researchers to continue to employ catenanes, in which symmetry has been broken, to design and synthesize artificial molecular motors.[161]

■ OUTLOOK

In contrast to the engineering and development of macroscopic man-made pumps and motors[24,25] which have taken place over millennia and the evolutionary refinement that has shaped their biological cousins, unrecognized, over the eons, artificial molecular pumps and motors[10] have only recently been subject to our creative design and contemporary synthesis. As a result, the artificial molecular pumps and motors thus far developed by scientists are primitive compared to their natural counterparts and have not yet begun to reach their full potential, but we have every reason to suspect that an ever-increasing number of applications will be developed. Gibbs thermodynamics played a critical role in the development of machines important in the industrial revolution. Similarly, we expect the trajectory thermodynamic approach,[69,133] based on Onsager's work,[33,34] further developed by Hill,[162] and set firmly on the foundation of microscopic reversibility,[19,20] to play a significant role in leading the design and creation of new molecular pumps and motors. Trajectory thermodynamics has already been key in unlocking the recognition that kinetic asymmetry,[38,132] and not only dissipation, plays a key role in both bio- and synthetic-molecular pumps and motors, as well as in fuel-driven assembly[135] and adaptation.[66,150−154] A key point is that catalytically driven molecular machines carry out their function by diffusion on a sculpted energy landscape. Synthetic chemists are nothing if not sculptors of the shapes of molecules, and concepts such as the pumping cassette, where emphasis is placed on the energy landscape created by a particular combination of chemical functional groups, and how that energy landscape can be modulated by catalysis or by changing the chemical makeup of the solution. When combined with autocatalytic processes, kinetic asymmetry may play a significant role in mechanisms by which simple matter becomes complex,[163] and even when it comes to attempts to create artificial life.[164]

Many of the early molecular rotors used chirality as the symmetry-breaking element, necessary to generate translation or rotation in one direction more than in another. Feringa[104] showed that an achiral molecule can be actuated by light to generate rotational motion, although this example involves two chiral helices (*P* and *M*) bonded together such that the molecule is not chiral. A different approach has been to use mechanically interlocked molecules designed to have broken symmetry in the plane of the molecule which is sufficient to allow pumping by an energy ratchet but does not require chirality.[165] The essential requirement is that the symmetry be broken in space and time,[166] i.e., that a molecular machine be designed with kinetic asymmetry.[38]

The pairing of mechanostereochemistry[167] with radical chemistry[137,168−171] in the past decade has proven powerful and allowed rings to be installed in rotaxanes and catenanes under non-equilibrium[135] conditions. For instance, a duet pump with a long collecting chain has allowed the synthesis of poly[*n*]rotaxanes,[147] unattainable by any synthetic approach conceived of prior to 2010.[137] Applications of the earliest artificial molecular pumps have been hampered by the irreversible nature of their operation. As a specific example of pumping to a high energy state and subsequently controlling relaxation, we have, in mechanically interlocked molecules, demonstrated two methods[142,143] for the capture and release of rings using artificial molecular pumps.

Artificial molecular motors also offer great potential for practical application, as shown[87] by systems such as the DNA-based molecular walker that can synthesize organic molecules as it progresses along a track. A catenane motor recently described in the literature[150] has demonstrated the possibility of catalysis-driven artificial molecular motors. It is expected that, as with rotaxane-based pumps, functionalization of the cargo—i.e., the rings—in such mechanically interlocked molecules will be the next step in unlocking the potential of these machines.

Taking cues from living systems, the use of artificial molecular machines for highly controlled synthesis is under investigation. Much in the way that the ribosome[172] translates information stored in RNA strands into the structure of peptides, rotaxane-based synthesizers have been reported by Leigh.[173−176] Given the complexity of biochemistry arising from a small handful of precursors, it seems likely that the sky is the limit for what can be created by these artificial systems.

Perhaps the greatest hurdle to harvesting the utility of artificial molecular pumps and motors is the imposition of long-range order over the system to effect meaningful change at the macroscopic level. Overcoming this obstacle by affixing such devices to surfaces or integrating them into membranes would open a new world of potential applications[10,15,111,112,177−180] for artificial molecular machines. Researchers looking for applications of artificial molecular machines have focused their attention on surfaces[113,114,181−184] porous crystals,[185−187] metal−organic frameworks,[115−117,188−197] and monolayers[198−201] of single molecules. Artificial molecular machines have been incorporated into liquid crystalline phases[202] and gels.[203−207] Motorized contractile gels have been developed by Giuseppone[205−210] who has integrated molecular motors into polymer chains. Medical science is set to benefit from artificial molecular machines acting as molecular prosthetics.[211−213]

With the numerous avenues for development available to artificial molecular pumps and motors, only time will tell what we can achieve in this new field of chemistry. Recently, the design and efficiency of these advanced artificial molecular machines have been improving rapidly, a trend which we can expect to continue. With this newfound control over the world of molecules, the next big thing is up to the reader as much as the authors of this Perspective.

■ AUTHOR INFORMATION

Corresponding Authors

R. Dean Astumian − *Department of Physics, University of Maine, Orono, Maine 04469, United States;* orcid.org/0000-0001-7472-187X; Email: astumian@maine.edu

J. Fraser Stoddart − *Department of Chemistry, Northwestern University, Evanston, Illinois 60208, United States; School of Chemistry, University of New South Wales, Sydney, NSW 2052, Australia; Stoddart Institute of Molecular Science, Department of Chemistry, Zhejiang University, Hangzhou 310027, China; ZJU-Hangzhou Global Scientific and*

Technological Innovation Center, Hangzhou 311215, China; orcid.org/0000-0003-3161-3697; Email: stoddart@northwestern.edu

Authors

Yuanning Feng − *Department of Chemistry, Northwestern University, Evanston, Illinois 60208, United States;* orcid.org/0000-0002-8832-0767

Marco Ovalle − *Department of Chemistry, Northwestern University, Evanston, Illinois 60208, United States*

James S. W. Seale − *Department of Chemistry, Northwestern University, Evanston, Illinois 60208, United States*

Christopher K. Lee − *School of Chemistry, University of New South Wales, Sydney, NSW 2052, Australia*

Dong Jun Kim − *School of Chemistry, University of New South Wales, Sydney, NSW 2052, Australia;* orcid.org/0000-0002-5930-1364

Complete contact information is available at: https://pubs.acs.org/10.1021/jacs.0c13388

Notes

The authors declare no competing financial interest.

ACKNOWLEDGMENTS

The authors would like to thank Northwestern University for its financial support.

REFERENCES

(1) Yannopoulos, S.; Lyberatos, G.; Theodossiou, N.; Li, W.; Valipour, M.; Tamburrino, A.; Angelakis, A. Evolution of Water Lifting Devices (Pumps) over the Centuries Worldwide. *Water* **2015**, *7*, 5031−5060.

(2) Vanhooydonck, D.; Symens, W.; Deprez, W.; Lemmens, J.; Stockman, K.; Dereyne, S. Calculating Energy Consumption of Motor Systems with Varying Load Using Iso Efficiency Contours. *The XIX International Conference on Electrical Machines - ICEM 2010*, Rome, Italy, Sept 6−8, 2010, IEEE, DOI: 10.1109/ICELMACH.2010.5607992.

(3) Ducklow, H. W.; Steinberg, D. K.; Buesseler, K. O. Upper Ocean Carbon Export and the Biological Pump. *Oceanography* **2001**, *14*, 50−58.

(4) Alberts, B.; Johnson, A.; Lewis, J.; Morgan, D.; Raff, M.; Roberts, K.; Walter, P.; Wilson, J. H.; Hunt, T. *Molecular Biology of the Cell*, 4th ed.; Garland Science, 2002.

(5) Astumian, R.; Derényi, I. Fluctuation Driven Transport and Models of Molecular Motors and Pumps. *Eur. Biophys. J.* **1998**, *27*, 474−489.

(6) (a) Wang, H.; Oster, G. Energy Transduction in the F_1 Motor of ATP Synthase. *Nature* **1998**, *396*, 279−282. (b) Toyabe, S.; Watanabe-Nakayama, T.; Okamoto, T.; Kudo, S.; Muneyuki, E. Thermodynamic Efficiency and Mechanochemical Coupling of F_1-ATPase. *Proc. Natl. Acad. Sci. U. S. A.* **2011**, *108*, 17951−17956.

(7) Feringa, B. L. The Art of Building Small: From Molecular Switches to Motors (Nobel Lecture). *Angew. Chem., Int. Ed.* **2017**, *56*, 11060−11078.

(8) Sauvage, J.-P. From Chemical Topology to Molecular Machines (Nobel Lecture). *Angew. Chem., Int. Ed.* **2017**, *56*, 11080−11093.

(9) Stoddart, J. F. Mechanically Interlocked Molecules (MIMs) - Molecular Shuttles, Switches, and Machines (Nobel Lecture). *Angew. Chem., Int. Ed.* **2017**, *56*, 11094−11125.

(10) (a) Balzani, V.; Gómez-López, M.; Stoddart, J. F. Molecular Machines. *Acc. Chem. Res.* **1998**, *31*, 405−414. (b) Balzani, V.; Credi, A.; Raymo, F. M.; Stoddart, J. F. Artificial Molecular Machines. *Angew. Chem., Int. Ed.* **2000**, *39*, 3348−3391. (c) Stoddart, J. F. Molecular Machines. *Acc. Chem. Res.* **2001**, *34*, 410−411. (d) Ballardini, R.; Balzani, V.; Credi, A.; Gandolfi, M. T.; Venturi, M. Artificial Molecular-Level Machines: Which Energy to Make Them Work? *Acc. Chem. Res.* **2001**, *34*, 445−455. (e) Kay, E. R.; Leigh, D. A.; Zerbetto, F. Synthetic Molecular Motors and Mechanical Machines. *Angew. Chem., Int. Ed.* **2007**, *46*, 72−191. (f) Coskun, A.; Banaszak, M.; Astumian, R. D.; Stoddart, J. F.; Grzybowski, B. A. Great Expectations: Can Artificial Molecular Machines Deliver on Their Promise? *Chem. Soc. Rev.* **2012**, *41*, 19−30. (g) Erbas-Cakmak, S.; Leigh, D. A.; McTernan, C. T.; Nussbaumer, A. L. Artificial Molecular Machines. *Chem. Rev.* **2015**, *115*, 10081−10206. (h) Kassem, S.; van Leeuwen, T.; Lubbe, A. S.; Wilson, M. R.; Feringa, B. L.; Leigh, D. A. Artificial Molecular Motors. *Chem. Soc. Rev.* **2017**, *46*, 2592−2621. (i) Wang, Q.; Chen, D.; Tian, H. Artificial Molecular Machines that can Perform Work. *Sci. China: Chem.* **2018**, *61*, 1261−1273. (j) Zhang, L.; Marcos, V.; Leigh, D. A. Molecular Machines with Bioinspired Mechanisms. *Proc. Natl. Acad. Sci. U. S. A.* **2018**, *115*, 9397−9404.

(11) Sengupta, S.; Spiering, M. M.; Dey, K. K.; Duan, W.; Patra, D.; Butler, P. J.; Astumian, R. D.; Benkovic, S. J.; Sen, A. DNA Polymerase as a Molecular Motor and Pump. *ACS Nano* **2014**, *8*, 2410−2418.

(12) Shapere, A.; Wilczek, F. Self-Propulsion at Low Reynolds Number. *Phys. Rev. Lett.* **1987**, *58*, 2051−2054.

(13) Curie, P. Sur la Symétrie dans les Phénomènes Physiques, Symétrie d'un Champ Électrique et d'un Champ Magnétique. *J. Phys. Theor. Appl.* **1894**, *3*, 393−415.

(14) Astumian, R. D. Design Principles for Brownian Molecular Machines: How to Swim in Molasses and Walk in a Hurricane. *Phys. Chem. Chem. Phys.* **2007**, *9*, 5067−5083.

(15) Kinbara, K.; Aida, T. Toward Intelligent Molecular Machines: Directed Motions of Biological and Artificial Molecules and Assemblies. *Chem. Rev.* **2005**, *105*, 1377−1400.

(16) (a) Leigh, D. A. Genesis of the Nanomachines: The 2016 Nobel Prize in Chemistry. *Angew. Chem., Int. Ed.* **2016**, *55*, 14506−14508. (b) Astumian, R. D. How Molecular Motors Work - Insights from the Molecular Machinist's Toolbox: The Nobel Prize in Chemistry 2016. *Chem. Sci.* **2017**, *8*, 840−845.

(17) Astumian, R. D. Optical vs. Chemical Driving for Molecular Machines. *Faraday Discuss.* **2016**, *195*, 583−597.

(18) (a) Einstein, A.; Ehrenfest, P. Zur Quantentheorie des Strahlungsgleichgewichts. *Eur. Phys. J. A* **1923**, *19*, 301−306. (b) Einstein, A. Die von der Molekularkinetischen Theorie der Wärme Gefordete Bewegung von in Ruhenden Flüssigkeiten Suspendierten Teilchen. *Ann. Phys.* **1905**, *4*, 549−560.

(19) Astumian, R. D. Microscopic Reversibility as the Organizing Principle of Molecular Machines. *Nat. Nanotechnol.* **2012**, *7*, 684−688. (b) Bier, M.; Derenyi, I.; Kostur, M.; Astumian, R. D. Intrawell Relaxation of Overdamped Brownian Particles. *Phys. Rev. E: Stat. Phys., Plasmas, Fluids, Relat. Interdiscip. Top.* **1999**, *59*, 6422−6432.

(20) Blackmond, D. G. If Pigs Could Fly" Chemistry: A Tutorial on the Principle of Microscopic Reversibility. *Angew. Chem., Int. Ed.* **2009**, *48*, 2648−2654.

(21) (a) Stoddart, J. F. The Chemistry of the Mechanical Bond. *Chem. Soc. Rev.* **2009**, *38*, 1802−1820. (b) Bruns, C. J.; Stoddart, J. F. *The Nature of the Mechanical Bond: From Molecules to Machines*; John Wiley & Sons Inc.: Hoboken, NJ, 2016.

(22) Barin, G.; Forgan, R. S.; Stoddart, J. F. Mechanostereochemistry and the Mechanical Bond. *Proc. R. Soc. London, Ser. A* **2012**, *468*, 2849−2880.

(23) (a) Baroncini, M.; Casimiro, L.; de Vet, C.; Groppi, J.; Silvi, S.; Credi, A. Making and Operating Molecular Machines: A Multidisciplinary Challenge. *ChemistryOpen* **2018**, *7*, 169−179. (b) Sluysmans, D.; Stoddart, J. F. Growing Community of Artificial Molecular Machinists. *Proc. Natl. Acad. Sci. U. S. A.* **2018**, *115*, 9359−9361. (c) Aprahamian, I. The Future of Molecular Machine. *ACS Cent. Sci.* **2020**, *6*, 347−358.

(24) (a) Tong, W. *Mechanical Design of Electric Motors*; CRC Press, 2014. (b) Hughes, A.; Drury, B. *Electric Motors and Drives*, 4th ed.; Elsevier, 2013.

(25) Frenning, L. *Pump Life Cycle Costs: A Guide to LCC Analysis for Pumping Systems*; Hydraulic Institite & Europump, 2001.

(26) Vogelesang, H. An Introduction to Energy Consumption in Pumps. *World Pumps* **2008**, *496*, 28−31.

(27) (a) Ducklow, H.; Steinberg, D.; Buesseler, K. Upper Ocean Carbon Export and the Biological Pump. *Oceanography* **2001**, *14*, 50−58. (b) Passow, U.; Carlson, C. The Biological Pump in a High CO_2 World. *Mar. Ecol.: Prog. Ser.* **2012**, *470*, 249−271.

(28) Saper, G.; Hess, H. Synthetic Systems Powered by Biological Molecular Motors. *Chem. Rev.* **2020**, *120*, 288−309.

(29) Qiu, Y.; Feng, Y.; Guo, Q.-H.; Astumian, R. D.; Stoddart, J. F. Pumps through the Ages. *Chem.* **2020**, *6*, 1952−1977.

(30) Mallouk, T. E.; Sen, A. How to Build Nanotech Motors. *Sci. Am.* **2009**, *300*, 72−77.

(31) Astumian, R. D. Making Molecules into Motors. *Sci. Am.* **2001**, *285*, 56−64.

(32) (a) Chandrasekhar, S. Brownian Motion, Dynamical Friction, and Stellar Dynamics. *Rev. Mod. Phys.* **1949**, *21*, 383−388. (b) Chandrasekhar, S. Stochastic Problems in Physics and Astronomy. *Rev. Mod. Phys.* **1943**, *15*, 1−89.

(33) (a) Onsager, L. Reciprocal Relations in Irreversible Processes. I. *Phys. Rev.* **1931**, *37*, 405−426. (b) Onsager, L. Reciprocal Relations in Irreversible Processes. II. *Phys. Rev.* **1931**, *38*, 2265−2279.

(34) Onsager, L.; Machlup, S. Fluctuations and Irreversible Processes. *Phys. Rev.* **1953**, *91*, 1505−1512.

(35) Purcell, E. M. Life at Low Reynolds Number. *Am. J. Phys.* **1977**, *45*, 3−11.

(36) Branscomb, E.; Russell, M. J. On the Beneficent Thickness of Water. *Interface Focus* **2019**, *9*, 20190061.

(37) Astumian, R. D.; Pezzato, C.; Feng, Y.; Qiu, Y.; McGonigal, P. R.; Cheng, C.; Stoddart, J. F. Non-Equilibrium Kinetics and Trajectory Thermodynamics of Synthetic Molecular Pumps. *Mater. Chem. Front.* **2020**, *4*, 1304−1314.

(38) Astumian, R. D. Kinetic Asymmetry Allows Macromolecular Catalysts to Drive an Information Ratchet. *Nat. Commun.* **2019**, *10*, 3837.

(39) Jencks, W. P. From Chemistry to Biochemistry to Catalysis to Movement. *Annu. Rev. Biochem.* **1997**, *66*, 1−18.

(40) (a) Jardetzky, O. Simple Allosteric Model for Membrane Pumps. *Nature* **1966**, *211*, 969−970. (b) Shimamura, T.; Weyand, S.; Beckstein, O.; Rutherford, N. G.; Hadden, J. M.; Sharples, D.; Sansom, M. S. P.; Iwata, S.; Henderson, P. J. F.; Cameron, A. D. Molecular Basis of Alternating Access Membrane Transport by the Sodium-Hydantoin Transporter Mhp1. *Science* **2010**, *328*, 470−473.

(41) Läuger, P. *Electrogenic Ion Pumps*; Oxford University Press, 1991.

(42) (a) Hwang, W.; Karplus, M. Structural Basis for Power Stroke vs. Brownian Ratchet Mechanisms of Motor Proteins. *Proc. Natl. Acad. Sci. U. S. A.* **2019**, *116*, 19777−19785. (b) Howard, J. Protein Power Strokes. *Curr. Biol.* **2006**, *16*, R517−R519.

(43) Sweeney, H. L.; Houdusse, A. Myosin VI Rewrites the Rules for Myosin Motors. *Cell* **2010**, *141*, 573−582.

(44) Astumian, R. D. Protein Conformational Fluctuations and Free-Energy Transduction. *Appl. Phys. A: Mater. Sci. Process.* **2002**, *75*, 193−206.

(45) (a) Chatterjee, M. N.; Kay, E. R.; Leigh, D. A. Beyond Switches: Ratcheting a Particle Energetically Uphill with a Compartmentalized Molecular Machine. *J. Am. Chem. Soc.* **2006**, *128*, 4058−4073. (b) von Delius, M.; Leigh, D. A. Walking Molecules. *Chem. Soc. Rev.* **2011**, *40*, 3656−3676.

(46) Reuss, L. *Seldin and Giebisch's The Kidney*, 5th ed.; Academic Press, 2008.

(47) (a) Dyla, M.; Hansen, S. B.; Nissen, P.; Kjaergaard, M. Structural Dynamics of P-Type ATPase Ion Pumps. *Biochem. Soc. Trans.* **2019**, *47*, 1247−1257. (b) Apell, H.-J. How Do P-Type ATPases Transport Ions? *Bioelectrochemistry* **2004**, *63*, 149−156. (c) Dyla, M.; Hansen, S. B.; Nissen, P.; Kjaergaard, M. Structural Dynamics of P-Type ATPase Ion Pumps. *Biochem. Soc. Trans.* **2019**, *47*, 1247−1257. (d) Stein, W. D.; Litman, T. *Channels, Carriers, and Pumps*, 2nd ed.; Academic Press, 2015.

(48) (a) Albers, R. W. Biochemical Aspects of Active Transport. *Annu. Rev. Biochem.* **1967**, *36*, 727−756. (b) Post, R. L.; Hegyvary, C.; Kume, S. Activation by Adenosine Triphosphate in the Phosphorylation Kinetics of Sodium and Potassium Ion Transport Adenosine Triphosphatase. *J. Biol. Chem.* **1972**, *247*, 6530−6540.

(49) Skou, J. C. The Influence of some Cations on an Adenosine Triphosphatase from Peripheral Nerves. *Biochim. Biophys. Acta* **1957**, *23*, 394−401.

(50) Skou, J. C. The Identification of the Sodium-Potassium Pump (Nobel Lecture). *Angew. Chem., Int. Ed.* **1998**, *37*, 2320−2328.

(51) (a) Kühlbrandt, W. Biology, Structure and Mechanism of P-Type ATPases. *Nat. Rev. Mol. Cell Biol.* **2004**, *5*, 282−295. (b) Apell, H.-J. How do P-type ATPases Transport Ions? *Bioelectrochemistry* **2004**, *63*, 149−156. (c) Bublitz, M.; Morth, J. P.; Nissen, P. P-Type ATPases at a Glance. *J. Cell Sci.* **2011**, *124*, 2515−2519. (d) Dyla, M.; Basse Hansen, S.; Nissen, P.; Kjaergaard, M. Structural Dynamics of P-Type ATPase Ion Pumps. *Biochem. Soc. Trans.* **2019**, *47*, 1247−1257.

(52) (a) Jencks, W. P. The Utilization of Binding Energy in Coupled Vectorial Processes. *Advances in Enzymology and Related Areas of Molecular Biology*; John Wiley & Sons Inc., 1980; pp 75−106. (b) Jencks, W. P. Utilization of Binding Energy and Coupling Rules for Active Transport and Other Coupled Vectorial Processes. *Methods in Enzymology*; Academic Press, 1989; pp 145−164.

(53) Branscomb, E.; Biancalani, T.; Goldenfeld, N.; Russell, M. Escapement Mechanisms and the Conversion of Disequilibria; *The Engines of Creation*. *Phys. Rep.* **2017**, *677*, 1−60.

(54) Carter, C. W., Jr High-Dimensional Mutant and Modular Thermodynamic Cycles, Molecular Switching, and Free Energy Transduction. *Annu. Rev. Biophys.* **2017**, *46*, 433−453.

(55) Carter, C. W., Jr Escapement Mechanisms: Efficient Free Energy Transduction by Reciprocally-Coupled Gating. *Proteins: Struct., Funct., Genet.* **2020**, *88*, 710−717.

(56) Koenig, F. O.; Horne, F. H.; Mohilner, D. M. On Thermodynamic Coupling of Chemical Reactions. *J. Am. Chem. Soc.* **1961**, *83*, 1029−1033.

(57) (a) Vale, R. D.; Milligan, R. A. The Way Things Move: Looking under the Hood of Molecular Motor Proteins. *Science* **2000**, *288*, 88−95. (b) van den Heuvel, M. G.; Dekker, C. Motor Proteins at Work for Nanotechnology. *Science* **2007**, *317*, 333−336.

(58) Iino, R.; Kinbara, K.; Bryant, Z. Introduction: Molecular Motors. *Chem. Rev.* **2020**, *120*, 1−4.

(59) (a) Kornberg, A. Biologic Synthesis of Deoxyribonucleic Acid. *Science* **1960**, *131*, 1503−1508. (b) Kornberg, R. The Molecular Basis of Eukaryotic Transcription (Nobel Lecture). *Angew. Chem., Int. Ed.* **2007**, *46*, 6956−6965.

(60) Mitchison, T.; Mitchison, H. How Cilia Beat. *Nature* **2010**, *463*, 308−309.

(61) Robert-Paganin, J.; Pylypenko, O.; Kikuti, C.; Sweeney, H. L.; Houdusse, A. Force Generation by Myosin Motors: A Structural Perspective. *Chem. Rev.* **2020**, *120*, 5−35.

(62) Pollard, T. D.; Korn, E. D. Acanthamoeba Myosin. I. Isolation from Acanthamoeba Castellanii of an Enzyme Similar to Muscle Myosin. *J. Biol. Chem.* **1973**, *248*, 4682−4690.

(63) (a) Szent-Györgyi, A. G. The Early History of the Biochemistry of Muscle Contraction. *J. Gen. Physiol.* **2004**, *123*, 631−641. (b) Oosawa, F. Discovery of Myosin I and Pollard-San. *Biophys. Rev.* **2018**, *10*, 1481−1482.

(64) (a) Sellers, J. R. Myosins: A Diverse Superfamily. *Biochim. Biophys. Acta, Mol. Cell Res.* **2000**, *1496*, 3−22. (b) Odronitz, F.; Kollmar, M. Drawing the Tree of Eukaryotic Life Based on the Analysis of 2,269 Manually Annotated Myosins from 328 Species. *Genome Biol.* **2007**, *8*, No. r196.

(65) Warshel, A. Bicycle-Pedal Model for the First Step in the Vision Process. *Nature* **1976**, *260*, 679−683.

(66) Astumian, R. D. Stochastically Pumped Adaptation and Directional Motion of Molecular Machines. *Proc. Natl. Acad. Sci. U. S. A.* **2018**, *115*, 9405−9413.

(67) Colquhoun, D.; Dowsland, K. A.; Beato, M.; Plested, A. J. How to Impose Microscopic Reversibility in Complex Reaction Mechanisms. *Biophys. J.* **2004**, *86*, 3510−3518.

(68) Astumian, R. D.; Chock, P. B.; Tsong, T. Y.; Chen, Y. D.; Westerhoff, H. V. Can Free Energy be Transduced from Electric Noise? *Proc. Natl. Acad. Sci. U. S. A.* **1987**, *84*, 434−438.

(69) Astumian, R. D.; Bier, M. Mechanochemical Coupling of the Motion of Molecular Motors to ATP Hydrolysis. *Biophys. J.* **1996**, *70*, 637−653.

(70) (a) Danowski, W.; van Leeuwen, T.; Browne, W. R.; Feringa, B. L. Photoresponsive Porous Materials. *Nanoscale Adv.* **2021**, *3*, 24−40. (b) Kistemaker, J. C. M.; Lubbe, A. S.; Feringa, B. L. Exploring Molecular Motors. *Mater. Chem. Front.* **2021**, DOI: 10.1039/D0QM01091J. (c) Costil, R.; Guinart, A.; Feringa, B. L. On the Right "Track" to Artificial Assemblers. *Chem* **2020**, *6*, 2868−2870.

(71) (a) Michaelis, L.; Menten, M. L. Die Kinetik der Invertinwirkung. *Biochem. Z.* **1913**, *49*, 333−369. (b) Michaelis, L.; Menten, M. L. *Die Kinetik der Invertinwirkung*; Universitätsbibliothek Johann Christian, Senckenberg, 2007. (c) Johnson, K. A.; Goody, R. S. The Original Michaelis Constant: Translation of the 1913 Michaelis-Menten Paper. *Biochemistry* **2011**, *50*, 8264−8269.

(72) (a) Astumian, R. D. Irrelevance of the Power-Stroke for the Directionality, Stopping Force, and Optimal Efficiency of Chemically Driven Molecular Machines. *Biophys. J.* **2015**, *108*, 291−303. (b) Astumian, R. D.; Mukherjee, S.; Warshel, A. The Physics and Physical Chemistry of Molecular Machines. *ChemPhysChem* **2016**, *17*, 1719−1741.

(73) Hill, T. L.; Eisenberg, E. Can Free Energy Transduction be Localized at some Crucial Part of the Enzymatic Cycle? *Q. Rev. Biophys.* **1981**, *14*, 463−511.

(74) (a) Mukherjee, S.; Warshel, A. Electrostatic Origin of the Unidirectionality of Walking Myosin V Motors. *Proc. Natl. Acad. Sci. U. S. A.* **2013**, *110*, 17326−17331. (b) Alhadeff, R.; Warshel, A. Reexamining the Origin of the Directionality of Myosin V. *Proc. Natl. Acad. Sci. U. S. A.* **2017**, *114*, 10426−10431. (c) Mukherjee, S.; Alhadeff, R.; Warshel, A. Simulating the Dynamics of the Mechanochemical Cycle of Myosin-V. *Proc. Natl. Acad. Sci. U. S. A.* **2017**, *114*, 2259−2264.

(75) Seifert, U. Stochastic Thermodynamics, Fluctuation Theorems and Molecular Machines. *Rep. Prog. Phys.* **2012**, *75*, 126001.

(76) (a) Mukherjee, S.; Warshel, A. Dissecting the Role of the γ-Subunit in the Rotary-Chemical Coupling and Torque Generation of F$_1$-ATPase. *Proc. Natl. Acad. Sci. U. S. A.* **2015**, *112*, 2746−2751. (b) Mukherjee, S.; Bora, R. P.; Warshel, A. Torque, Chemistry and Efficiency in Molecular Motors: A Study of the Rotary-Chemical Coupling in F$_1$-ATPase. *Q. Rev. Biophys.* **2015**, *48*, 395−403.

(77) Bai, C.; Warshel, A. Revisiting the Protomotive Vectorial Motion of F$_o$-ATPase. *Proc. Natl. Acad. Sci. U. S. A.* **2019**, *116*, 19484−19489.

(78) Abrahams, J. P.; Leslie, A. G. W.; Lutter, R.; Walker, J. E. Structure at 2.8 Å Resolution of F$_1$-ATPase from Bovine Heart Mitochondria. *Nature* **1994**, *370*, 621−628.

(79) Boyer, P. D. The Binding Change Mechanism for ATP Synthase—Some Probabilities and Possibilities. *Biochim. Biophys. Acta, Bioenerg.* **1993**, *1140*, 215−250.

(80) (a) Capaldi, R. A.; Aggeler, R. Mechanism of the F$_1$F$_o$-Type ATP Synthase, a Biological Rotary Motor. *Trends Biochem. Sci.* **2002**, *27*, 154−160. (b) Bublitz, M.; Morth, J. P.; Nissen, P. P-Type ATPases at a Glance. *J. Cell Sci.* **2011**, *124*, 2515−2519. (c) Stewart, A. G.; Sobti, M.; Harvey, R. P.; Stock, D. Rotary ATPases. *BioArchitecture* **2013**, *3*, 2−12. (d) Neupane, P.; Bhuju, S.; Thapa, N.; Bhattarai, H. K. ATP Synthase: Structure, Function and Inhibition. *Biomol. Concepts* **2019**, *10*, 1−10.

(81) (a) de la Cruz, E. M.; Wells, A. L.; Rosenfeld, S. S.; Ostap, E. M.; Sweeney, H. L. The Kinetic Mechanism of Myosin V. *Proc. Natl. Acad. Sci. U. S. A.* **1999**, *96*, 13726−13731. (b) Mehta, A. D.; Rock, R. S.; Rief, M.; Spudich, J. A.; Mooseker, M. S.; Cheney, R. E. Myosin-V is a Processive Actin-Based Motor. *Nature* **1999**, *400*, 590−593. (c) Ito, K.; Ikebe, M.; Kashiyama, T.; Mogami, T.; Kon, T.; Yamamoto, K. Kinetic Mechanism of the Fastest Motor Protein, *Chara* Myosin. *J. Biol. Chem.* **2007**, *282*, 19534−19545.

(82) Derenyi, I.; Bier, M.; Astumian, R. D. Generalized Efficiency and its Application to Microscopic Engines. *Phys. Rev. Lett.* **1999**, *83*, 903−906.

(83) Noji, H.; Yasuda, R.; Yoshida, M.; Kinosita, K. Direct Observation of the Rotation of F$_1$-ATPase. *Nature* **1997**, *386*, 299−302.

(84) Boyer, P. D. Energy, Life, and ATP (Nobel Lecture). *Angew. Chem., Int. Ed.* **1998**, *37*, 2296−2307.

(85) Soong, R. K.; Bachand, G. D.; Neves, H. P.; Olkhovets, A. G.; Craighead, H. G.; Montemagno, C. Powering an Inorganic Nanodevice with a Biomolecular Motor. *Science* **2000**, *290*, 1555−1558.

(86) (a) Shin, J.-S.; Pierce, N. A. A Synthetic DNA Walker for Molecular Transport. *J. Am. Chem. Soc.* **2004**, *126*, 10834−10835. (b) Sherman, W. B.; Seeman, N. C. A Precisely Controlled DNA Biped Walking Device. *Nano Lett.* **2004**, *4*, 1203−1207. (c) Yin, P.; Yan, H.; Daniell, X. G.; Turberfield, A. J.; Reif, J. H. A Unidirectional DNA Walker that Moves Autonomously along a Track. *Angew. Chem., Int. Ed.* **2004**, *43*, 4906−4911. (d) Tian, Y.; He, Y.; Chen, Y.; Yin, P.; Mao, C. A DNAzyme that Walks Processively and Autonomously along a One-Dimensional Track. *Angew. Chem., Int. Ed.* **2005**, *44*, 4355−4358. (e) Pei, R.; Taylor, S. K.; Stefanovic, D.; Rudchenko, S.; Mitchell, T. E.; Stojanovic, M. N. Behavior of Polycatalytic Assemblies in a Substrate-Displaying Matrix. *J. Am. Chem. Soc.* **2006**, *128*, 12693−12699. (f) Yin, P.; Choi, H. M. T.; Calvert, C. R.; Pierce, N. A. Programming Biomolecular Self-Assembly Pathways. *Nature* **2008**, *451*, 318−322. (g) Green, S. J.; Bath, J.; Turberfield, A. J. Coordinated Chemomechanical Cycles: A Mechanism for Autonomous Molecular Motion. *Phys. Rev. Lett.* **2008**, *101*, 238101.

(87) Omabegho, T.; Sha, R.; Seeman, N. C. A Bipedal DNA Brownian Motor with Coordinated Legs. *Science* **2009**, *324*, 67−71.

(88) He, Y.; Liu, D. Autonomous Multistep Organic Synthesis in a Single Isothermal Solution Mediated by a DNA Walker. *Nat. Nanotechnol.* **2010**, *5*, 778−782.

(89) Ramezani, H.; Dietz, H. Building Machines with DNA Molecules. *Nat. Rev. Genet.* **2020**, *21*, 5−26.

(90) The first artificial small-molecule walker was reported by Leigh.[91] In a departure from the non-covalent DNA-based walkers popular in the preceding period, this system uses an orthogonal pair of reversible covalent bonds which, coupled with sequential pH changes, allows unidirectional motion of the walker along its track. This small-molecule walker contains just 21 atoms and has a step size of 1.4 nm on its four-foothold track, notably smaller than kinesin, a 250 kD protein walker which takes 16.6 nm steps. Unlike kinesin, however, this walker does not capture, transport, or release molecular cargo. A goal is to obtain an artificial molecular walker that can move cargo along polymeric and/or surface-bound tracks in a unidirectional and autonomous fashion.

(91) (a) von Delius, M.; Geertsema, E.; Leigh, D. A. A Synthetic Small Molecule that can Walk down a Track. *Nat. Chem.* **2010**, *2*, 96−101. (b) von Delius, M.; Geertsema, E. M.; Leigh, D. A.; Tang, D.-T. D. Design, Synthesis, and Operation of Small Molecules That Walk along Tracks. *J. Am. Chem. Soc.* **2010**, *132*, 16134−16145.

(92) Mohapatra, S.; Lin, C.-T.; Feng, X. A.; Basu, A.; Ha, T. Single-Molecule Analysis and Engineering of DNA Motors. *Chem. Rev.* **2020**, *120*, 36−78.

(93) (a) Goel, A.; Vogel, V. Harnessing Biological Motors to Engineer Systems for Nanoscale Transport and Assembly. *Nat. Nanotechnol.* **2008**, *3*, 465−475. (b) Lipowsky, R.; Klumpp, S.; Nieuwenhuizen, T. M. Random Walks of Cytoskeletal Motors in Open and Closed Compartments. *Phys. Rev. Lett.* **2001**, *87*, 108101. (c) Hameroff, S. R.; Dayhoff, J. E.; Lahoz-Beltra, R.; Samsonovich, A. V.; Rasmussen, S. Models for Molecular Computation: Conformational Automata in the Cytoskeleton. *Computer* **1992**, *25*, 30−39. (d) Nicolau, D. V. Dynamic Nanodevices Based on Protein Molecular

Motors. In *BioMEMS and Biomedical Nanotechnology*; Ferrari, M., Lee, A. P., Lee, L. J., Eds.; Springer, 2006.

(94) Howe, E. N. W.; Gale, P. A. Fatty Acid Fueled Transmembrane Chloride Transport. *J. Am. Chem. Soc.* **2019**, *141*, 10654−10660.

(95) Feynman, R. P. There's Plenty of Room at the Bottom. *Engineering and Science* **1960**, *23*, 22−36.

(96) Gale, P. A.; Davis, J. T.; Quesada, R. Anion Transport and Supramolecular Medicinal Chemistry. *Chem. Soc. Rev.* **2017**, *46*, 2497−2519.

(97) Weiss, R. M.; Warshel, A. A New View of the Dynamics of Singlet Cis-Trans Photoisomerization. *J. Am. Chem. Soc.* **1979**, *101*, 6131−6133.

(98) (a) Feringa, B.; Wynberg, H. Torsionally Distorted Olefins. Resolution of *cis*- and *trans*-4,4′-Bi-1,1′,2,2′,3,3′-hexahydrophenanthrylidene. *J. Am. Chem. Soc.* **1977**, *99*, 602−603. (b) Feringa, B. L.; Jager, W. F.; de Lange, B.; Meijer, E. W. Chiroptical Molecular Switch. *J. Am. Chem. Soc.* **1991**, *113*, 5468−5470.

(99) Ruangsupapichat, N.; Pollard, M. M.; Harutyunyan, S. R.; Feringa, B. L. Reversing the Direction in a Light-Driven Rotary Molecular Motor. *Nat. Chem.* **2011**, *3*, 53−60.

(100) Here *P* denotes the right-handed helicity in each half of the structure; *M*, used later, stands for left-handed helicity.

(101) Feringa, B. L. In Control of Motion: From Molecular Switches to Molecular Motors. *Acc. Chem. Res.* **2001**, *34*, 504−513.

(102) Koumura, N.; Geertsema, E. M.; van Gelder, M. B.; Meetsma, A.; Feringa, B. L. Second Generation Light-Driven Molecular Motors. Unidirectional Rotation Controlled by a Single Stereogenic Center with Near-Perfect Photoequilibria and Acceleration of the Speed of Rotation by Structural Modification. *J. Am. Chem. Soc.* **2002**, *124*, 5037−5051.

(103) Kistemaker, J. C.; Štacko, P.; Roke, D.; Wolters, A. T.; Heideman, G. H.; Chang, M.-C.; van der Meulen, P.; Visser, J.; Otten, E.; Feringa, B. L. Third-Generation Light-Driven Symmetric Molecular Motors. *J. Am. Chem. Soc.* **2017**, *139*, 9650−9661.

(104) Kistemaker, J. C. M.; Štacko, P.; Visser, J.; Feringa, B. L. Unidirectional Rotary Motion in Achiral Molecular Motors. *Nat. Chem.* **2015**, *7*, 890−896.

(105) Vicario, J.; Walko, M.; Meetsma, A.; Feringa, B. L. Fine Tuning of the Rotary Motion by Structural Modification in Light-Driven Unidirectional Molecular Motors. *J. Am. Chem. Soc.* **2006**, *128*, 5127−5135.

(106) Conyard, J.; Addison, K.; Heisler, I. A.; Cnossen, A.; Browne, W. R.; Feringa, B. L.; Meech, S. R. Ultrafast Dynamics in the Power Stroke of a Molecular Rotary Motor. *Nat. Chem.* **2012**, *4*, 547−551.

(107) Miller, R. J. D. Molecular Motor Speed Limits. *Nat. Chem.* **2012**, *4*, 523−525.

(108) Koumura, N.; Zijlstra, R. W. J.; van Delden, R. A.; Harada, N.; Feringa, B. L. Light-Driven Monodirectional Molecular Rotor. *Nature* **1999**, *401*, 152−155.

(109) Geertsema, E. M.; van der Molen, S. J.; Martens, M.; Feringa, B. L. Optimizing Rotary Processes in Synthetic Molecular Motors. *Proc. Natl. Acad. Sci. U. S. A.* **2009**, *106*, 16919−16924.

(110) van Leeuwen, T.; Lubbe, A. S.; Štacko, P.; Wezenberg, S. J.; Feringa, B. L. Dynamic Control of Function by Light-Driven Molecular Motors. *Nat. Rev. Chem.* **2017**, *1*, 0096.

(111) Zhang, Q.; Qu, D.-H.; Tian, H.; Feringa, B. L. Bottom-Up: Can Supramolecular Tools Deliver Responsiveness from Molecular Motors to Macroscopic Materials? *Matter* **2020**, *3*, 355−370.

(112) Feringa, B. L. Vision Statement: Materials in Motion. *Adv. Mater.* **2020**, *32*, 1906416.

(113) van Delden, R. A.; ter Wiel, M. K. J.; Pollard, M. M.; Vicario, J.; Koumura, N.; Feringa, B. L. Unidirectional Molecular Motor on a Gold Surface. *Nature* **2005**, *437*, 1337−1340.

(114) Browne, W. R.; Feringa, B. L. Making Molecular Machines Work. *Nat. Nanotechnol.* **2006**, *1*, 25−35.

(115) Danowski, W.; van Leeuwen, T.; Abdolahzadeh, S.; Roke, D.; Browne, W. R.; Wezenberg, S. J.; Feringa, B. L. Unidirectional Rotary Motion in a Metal-Organic Framework. *Nat. Nanotechnol.* **2019**, *14*, 488−494.

(116) Krause, S.; Feringa, B. L. Towards Artificial Molecular Factories from Framework-Embedded Molecular Machines. *Nat. Rev. Chem.* **2020**, *4*, 550−562.

(117) Danowski, W.; Castiglioni, F.; Sardjan, A. S.; Krause, S.; Pfeifer, L.; Roke, D.; Comotti, A.; Browne, W. R.; Feringa, B. L. Visible-Light-Driven Rotation of Molecular Motors in a Dual-Function Metal-Organic Framework Enabled by Energy Transfer. *J. Am. Chem. Soc.* **2020**, *142*, 9048−9056.

(118) Greb, L.; Lehn, J.-M. Light-Driven Molecular Motors: Imines as Four-Step or Two-Step Unidirectional Rotors. *J. Am. Chem. Soc.* **2014**, *136*, 13114−13117.

(119) (a) Su, X.; Robbins, T. F.; Aprahamian, I. Switching Through Coordination-Coupled Proton Transfer. *Angew. Chem., Int. Ed.* **2011**, *50*, 1841−1844. (b) Yang, Y.; Hughes, R. P.; Aprahamian, I. Visible Light Switching of a BF_2-Coordinated Azo Compound. *J. Am. Chem. Soc.* **2012**, *134*, 15221−15224. (c) Aprahamian, I. Molecules Bearing Robotic Arms. *Nat. Chem.* **2016**, *8*, 97−99. (d) Aprahamian, I. Hydrazone Switches and Things in Between. *Chem. Commun.* **2017**, *53*, 6674−6684.

(120) Ragazzon, G.; Baroncini, M.; Silvi, S.; Venturi, M.; Credi, A. Light-Powered Autonomous and Directional Molecular Motion of a Dissipative Self-Assembling System. *Nat. Nanotechnol.* **2015**, *10*, 71−75.

(121) Muller, P. Glossary of Terms Used in Physical Organic Chemistry (IUPAC Recommendations 1994). *Pure Appl. Chem.* **1994**, *66*, 1077−1184.

(122) Glink, P. T.; Schiavo, C.; Stoddart, J. F.; Williams, D. J. The Genesis of a New Range of Interlocked Molecules. *Chem. Commun.* **1996**, *13*, 1483−1490.

(123) Groppi, J.; Baroncini, M.; Venturi, M.; Silvi, S.; Credi, A. Design of Photo-Activated Molecular Machines: Highlights from the Past Ten Years. *Chem. Commun.* **2019**, *55*, 12595−12602.

(124) Corra, S.; Curcio, M.; Baroncini, M.; Silvi, S.; Credi, A. Photoactivated Artificial Molecular Machines that Can Perform Tasks. *Adv. Mater.* **2020**, *32*, 1906064.

(125) Baroncini, M.; Silvi, S.; Credi, A. Photo- and Redox-Driven Artificial Molecular Motors. *Chem. Rev.* **2020**, *120*, 200−268.

(126) (a) Tierney, H. L.; Murphy, C. J.; Jewell, A. D.; Baber, A. E.; Iski, E. V.; Khodaverdian, H. Y.; McGuire, A. F.; Klebanov, N.; Sykes, E. C. H. Experimental Demonstration of a Single-Molecule Electric Motor. *Nat. Nanotechnol.* **2011**, *6*, 625−629. (b) Michl, J.; Sykes, E. C. H. Molecular Rotors and Motors: Recent Advances and Future Challenges. *ACS Nano* **2009**, *3*, 1042−1048. (c) Kottas, G. S.; Clarke, L. I.; Horinek, D.; Michl, J. Artificial Molecular Rotors. *Chem. Rev.* **2005**, *105*, 1281−1376.

(127) Onsager, L. The Motion of Ions: Principles and Concepts. *Science* **1969**, *166*, 1359−1364.

(128) van Houten, J. A Century of Chemical Dynamics Traced through the Nobel Prizes. 1967: Eigen, Norrish, and Porter. *J. Chem. Educ.* **2002**, *79*, 548−550.

(129) Norrish, R. Some Fast Reactions in Gases Studied by Flash Photolysis and Kinetic Spectroscopy. *Spectroscopy of the Excited State*; Springer, 1976; pp 117−160.

(130) Porter, G. Flash Photolysis and some of its Applications. *Science* **1968**, *160*, 1299−1307.

(131) Eigen, M. Immeasurably Fast Reactions, Nobel Lecture, Dec 11, 1967.

(132) Astumian, R. D.; Robertson, B. Imposed Oscillations of Kinetic Barriers can Cause an Enzyme to Drive a Chemical Reaction away from Equilibrium. *J. Am. Chem. Soc.* **1993**, *115*, 11063−11068.

(133) (a) Astumian, R. D. Thermodynamics and Kinetics of Molecular Motors. *Biophys. J.* **2010**, *98*, 2401−2409. (b) Astumian, R. D. Trajectory and Cycle-Based Thermodynamics and Kinetics of Molecular Machines: The Importance of Microscopic Reversibility. *Acc. Chem. Res.* **2018**, *51*, 2653−2661.

(134) Li, H.; Cheng, C.; McGonigal, P. R.; Fahrenbach, A. C.; Frasconi, M.; Liu, W.-G.; Zhu, Z.; Zhao, Y.; Ke, C.; Lei, J.; Young, R. M.; Dyar, S. M.; Co, D. T.; Yang, Y.-W.; Botros, Y. Y.; Goddard, W. A., III; Wasielewski, M. R.; Astumian, R. D.; Stoddart, J. F. Relative

Unidirectional Translation in an Artificial Molecular Assembly Fueled by Light. *J. Am. Chem. Soc.* **2013**, *135*, 18609−18620.

(135) Pezzato, C.; Cheng, C.; Stoddart, J. F.; Astumian, R. D. Mastering the Non-Equilibrium Assembly and Operation of Molecular Machines. *Chem. Soc. Rev.* **2017**, *46*, 5491−5507.

(136) Cheng, C.; McGonigal, P. R.; Liu, W.-G.; Li, H.; Vermeulen, N. A.; Ke, C.; Frasconi, M.; Stern, C. L.; Goddard, W. A., III; Stoddart, J. F. Energetically Demanding Transport in a Supramolecular Assembly. *J. Am. Chem. Soc.* **2014**, *136*, 14702−14705.

(137) (a) Trabolsi, A.; Khashab, N.; Fahrenbach, A. C.; Friedman, D. C.; Colvin, M. T.; Cotí, K. K.; Benítez, D.; Tkatchouk, E.; Olsen, J. C.; Belowich, M. E.; Carmielli, R.; Khatib, H. A.; Goddard, W. A., III; Wasielewski, M. R.; Stoddart, J. F. Radically Enhanced Molecular Recognition. *Nat. Chem.* **2010**, *2*, 42−49. (b) Fahrenbach, A. C.; Barnes, J. C.; Lanfranchi, D. A.; Li, H.; Coskun, A.; Gassensmith, J. J.; Liu, Z.; Benítez, D.; Trabolsi, A.; Goddard, W. A., III; Elhabiri, M.; Stoddart, J. F. Solution-Phase Mechanistic Study and Solid-State Structure of a Tris(bipyridinium Radical Cation) Inclusion Complex. *J. Am. Chem. Soc.* **2012**, *134*, 3061−3072.

(138) BIPY is the abbreviation of 4,4′-bipyridinium, which in other publications is denoted as viologen (V).

(139) (a) Cheng, C.; McGonigal, P. R.; Schneebeli, S. T.; Li, H.; Vermeulen, N. A.; Ke, C.; Stoddart, J. F. An Artificial Molecular Pump. *Nat. Nanotechnol.* **2015**, *10*, 547−553. (b) Cheng, C.; McGonigal, P. R.; Stoddart, J. F.; Astumian, R. D. Design and Synthesis of Nonequilibrium Systems. *ACS Nano* **2015**, *9*, 8672−8688.

(140) Pezzato, C.; Nguyen, M. T.; Cheng, C.; Kim, D. J.; Otley, M. T.; Stoddart, J. F. An Efficient Artificial Molecular Pump. *Tetrahedron* **2017**, *73*, 4849−4857.

(141) The Mark I[139] and Mark II[140] AMPs share a similar design but with different pumping cassettes. In contrast to the Mark I AMP, which uses a cationic 3,5-dimethylpyridinium electrostatic barrier, the Mark II employs a cationic 2,6-dimethylpyridinium (PY^+) electrostatic barrier, with its methyl groups pointing toward the nearby bipyridinium ($BIPY^{2+}$) unit, creating higher steric bulk close to the zone of maximum Coulombic repulsion. In addition, the IPP steric barrier is connected to the $BIPY^{2+}$ by a methylene linker, which is shorter than the bismethylene linker used in the Mark I AMP. As a result of these modifications, the Mark II AMP is more efficient because of the compactness of the pumping cassette compared to that in the Mark I.

(142) Qiu, Y.; Zhang, L.; Pezzato, C.; Feng, Y.; Li, W.; Nguyen, M. T.; Cheng, C.; Shen, D.; Guo, Q.-H.; Shi, Y.; Cai, K.; Alsubaie, F. M.; Astumian, R. D.; Stoddart, J. F. A Molecular Dual Pump. *J. Am. Chem. Soc.* **2019**, *141*, 17472−17476.

(143) Guo, Q.-H.; Qiu, Y.; Kuang, X.; Liang, J.; Feng, Y.; Zhang, L.; Jiao, Y.; Shen, D.; Astumian, R. D.; Stoddart, J. F. Artificial Molecular Pump Operating in Response to Electricity and Light. *J. Am. Chem. Soc.* **2020**, *142*, 14443−14449.

(144) (a) Hansen, M. J.; Velema, W. A.; Lerch, M. M.; Szymanski, W.; Feringa, B. L. Wavelength-Selective Cleavage of Photoprotecting Groups: Strategies and Applications in Dynamic Systems. *Chem. Soc. Rev.* **2015**, *44*, 3358−3377. (b) Patchornik, A.; Amit, B.; Woodward, R. B. Photosensitive Protecting Groups. *J. Am. Chem. Soc.* **1970**, *92*, 6333−6335.

(145) (a) Tsong, T. Y.; Astumian, R. D. Electroconformational Coupling and Membrane Protein Function. *Prog. Biophys. Mol. Biol.* **1987**, *50*, 1−45. (b) Boyer, P. D. A Perspective of the Binding Change Mechanism for ATP Synthesis. *FASEB J.* **1989**, *3*, 2164−2178.

(146) Chen, S.; Wang, Y.; Nie, T.; Bao, C.; Wang, C.; Xu, T.; Lin, Q.; Qu, D.-H.; Gong, X.; Yang, Y.; Zhu, L.; Tian, H. An Artificial Molecular Shuttle Operates in Lipid Bilayers for Ion Transport. *J. Am. Chem. Soc.* **2018**, *140*, 17992−17998.

(147) Qiu, Y.; Song, B.; Pezzato, C.; Shen, D.; Liu, W.; Zhang, L.; Feng, Y.; Guo, Q.-H.; Cai, K.; Li, W.; Chen, H.; Nguyen, M. T.; Shi, Y.; Cheng, C.; Astumian, R. D.; Li, X.; Stoddart, J. F. A Precise Polyrotaxane Synthesizer. *Science* **2020**, *368*, 1247−1253.

(148) The pumping cassette is designed to have an energy well (e.g., $BIPY^{\bullet+}$) surrounded by two barriers (e.g., PY^+ and IPP), where the energy of the well and the energy of at least one barrier can be modulated externally. The direction of the pumping of a $\mathbf{CBPQT^{4+}}$ ring as it undergoes redox cycles is from $PY^+ \rightarrow BIPY^{\bullet+}/BIPY^{2+} \rightarrow$ IPP. When the IPP steric barrier is between the recognition site and the collecting chain, we say that the cassette is inward facing, and when the IPP is between the recognition site and the bulk solution, we say that the cassette is outward facing. In a molecular dual pump,[142] two pumping cassettes are arranged such that one is inward facing and the other is outward facing. A duet pump[149] (originally referred to as a "dual molecular pump"), in which both pumping cassettes are arranged in an inward-facing fashion, has also been demonstrated. The flexibility of arranging the pumping cassettes offers great versatility with respect to designing AMMs.

(149) Pezzato, C.; Nguyen, M. T.; Kim, D. J.; Anamimoghadam, O.; Mosca, L.; Stoddart, J. F. Controlling Dual Molecular Pumps Electrochemically. *Angew. Chem., Int. Ed.* **2018**, *57*, 9325−9329.

(150) Te Brinke, E.; Groen, J.; Herrmann, A.; Heus, H. A.; Rivas, G.; Spruijt, E.; Huck, W. T. Dissipative Adaptation in Driven Self-Assembly Leading to Self-Dividing Fibrils. *Nat. Nanotechnol.* **2018**, *13*, 849−855.

(151) Rieß, B.; Grötsch, R. K.; Boekhoven, J. The Design of Dissipative Molecular Assemblies Driven by Chemical Reaction Cycles. *Chem.* **2020**, *6*, 552−578.

(152) De, S.; Klajn, R. Dissipative Self-Assembly Driven by the Consumption of Chemical Fuels. *Adv. Mater.* **2018**, *30*, 1706750.

(153) Post, E.; Fletcher, S. P. Dissipative Self-Assembly, Competition and Inhibition in a Self-Reproducing Protocell Model. *Chem. Sci.* **2020**, *11*, 9434−9442.

(154) Singh, N.; Formon, G. J. M.; de Piccoli, S.; Hermans, T. M. Devising Synthetic Reaction Cycles for Dissipative Nonequilibrium Self-Assembly. *Adv. Mater.* **2020**, *32*, 1906834.

(155) Wilson, M. R.; Solà, J.; Carlone, A.; Goldup, S. M.; Lebrasseur, N.; Leigh, D. A. An Autonomous Chemically Fuelled Small-Molecule Motor. *Nature* **2016**, *534*, 235−240.

(156) The fumaramide (**Fum**) recognition site (Figure 11) at the bottom is deuterated for NMR spectroscopic analysis.

(157) Serreli, V.; Lee, C.-F.; Kay, E. R.; Leigh, D. A. A Molecular Information Ratchet. *Nature* **2007**, *445*, 523−527.

(158) Leigh, D. A.; Wong, J. K. Y.; Dehez, F.; Zerbetto, F. Unidirectional Rotation in a Mechanically Interlocked Molecular Rotor. *Nature* **2003**, *424*, 174−179.

(159) Hernández, J. V.; Kay, E. R.; Leigh, D. A. A Reversible Synthetic Rotary Molecular Motor. *Science* **2004**, *306*, 1532−1537.

(160) Erbas-Cakmak, S.; Fielden, S. D. P.; Karaca, U.; Leigh, D. A.; McTernan, C. T.; Tetlow, D. J.; Wilson, M. R. Rotary and Linear Molecular Motors Driven by Pulses of a Chemical Fuel. *Science* **2017**, *358*, 340−343.

(161) Borsley, S.; Leigh, D. A.; Roberts, B. M. W. A Doubly Kinetically-Gated Information Ratchet Autonomously Driven by Carbodiimide Hydration. *J. Am. Chem. Soc.* **2021**, *143*, 4414−4420.

(162) (a) Hill, T. L. The Linear Onsager Coefficients for Biochemical Kinetic Diagrams as Equilibrium One-Way Cycle Fluxes. *Nature* **1982**, *299*, 84−86. (b) Eisenberg, E.; Hill, T. L. Muscle Contraction and Free Energy Transduction in Biological Systems. *Science* **1985**, *227*, 999−1006.

(163) Lehn, J.-M. Perspectives in Chemistry—Steps towards Complex Matter. *Angew. Chem., Int. Ed.* **2013**, *52*, 2836−2850.

(164) Pross, A. *What is Life: How Chemistry Becomes Biology*; Oxford University Press, 2012.

(165) Astumian, R. D. Chemical Peristalsis. *Proc. Natl. Acad. Sci. U. S. A.* **2005**, *102*, 1843−1847.

(166) Astumian, R. D. Symmetry Relations for Trajectories of a Brownian Motor. *Phys. Rev. E* **2007**, *76*, 020102.

(167) (a) Olson, M. A.; Botros, Y. Y.; Stoddart, J. F. Mechanostereochemistry. *Pure Appl. Chem.* **2010**, *82*, 1569−1574. (b) Barin, G.; Forgan, R. S.; Stoddart, J. F. Mechanostereochemistry

and the Mechanical Bond. *Proc. Math. Phys. Eng. Sci.* **2012**, *468*, 2849−2880.

(168) In the design of molecular machines, a key feature that distinguishes radical pairing from other switchable recognition motifs is the greater strength of radical−radical interactions. Although the fact that radical viologens form dimers (referred to as pimers by Hünig[169]) had long been established in the literature,[170] it was not until 2010 that we showed[137] that such radical pairing could be leveraged to build complex molecular architectures. The first tristable rotaxane was reported in which the residence of a CBPQT^{4+} ring at one of three stations in the rotaxane could be controlled by changing the oxidation state of the compound. A free energy of binding of −17 kcal mol^{-1} was determined[137] for the BIPY$^{\bullet+}\subset$CBPQT$^{2(\bullet+)}$ trisradical tricationic complex. This value, approximately 20% the strength of a carbon−carbon single bond, is especially remarkable considering that the complex is formed by bringing two cationic species into close proximity. The Coulombic repulsion between the CBPQT^{4+} ring and BIPY^{2+} is[171] ca. 15 kcal mol^{-1}. Consequently, each redox cycle is able to utilize approximately 32 kcal mol^{-1} for doing work, e.g., for pumping.

(169) (a) Hünig, S. Stable Radical Ions. *Pure Appl. Chem.* **1967**, *15*, 109−122. (b) Geuder, W.; Hünig, S.; Suchy, A. Single and Double Bridged Viologenes and Intramolecular Pimerization of their Cation Radicals. *Tetrahedron* **1986**, *42*, 1665−1677. (c) Geraskina, M. R.; Dutton, A. S.; Juetten, M. J.; Wood, S. A.; Winter, A. H. The Viologen Cation Radical Pimer: A Case of Dispersion-Driven Bonding. *Angew. Chem., Int. Ed.* **2017**, *56*, 9435−9439.

(170) Kosower, E. M.; Cotter, J. L. Stable Free Radicals. II. The Reduction of 1-Methyl-4-cyanopyridinium Ion to Methylviologen Cation Radical. *J. Am. Chem. Soc.* **1964**, *86*, 5524−5527.

(171) Cai, K.; Zhang, L.; Astumian, R. D.; Stoddart, J. F. Radical-Pairing Induced Molecular Assembly and Motion. *Nat. Rev. Chem.* **2021**, in press.

(172) (a) Moore, P. B. How Should We Think About the Ribosome? *Annu. Rev. Biophys.* **2012**, *41*, 1−19. (b) Frank, J.; Gonzalez, R. L., Jr. Structure and Dynamics of a Processive Brownian Motor: The Translating Ribosome. *Annu. Rev. Biochem.* **2010**, *79*, 381−412.

(173) Lewandowski, B.; De Bo, G.; Ward, J. W.; Papmeyer, M.; Kuschel, S.; Aldegunde, M. J.; Gramlich, P. M. E.; Heckmann, D.; Goldup, S. M.; D'Souza, D. M.; Fernandes, A. E.; Leigh, D. A. Sequence-Specific Peptide Synthesis by an Artificial Small-Molecule Machine. *Science* **2013**, *339*, 189−193.

(174) de Bo, G.; Gall, M. A. Y.; Kitching, M. O.; Kuschel, S.; Leigh, D. A.; Tetlow, D. J.; Ward, J. W. Sequence-Specific β-Peptide Synthesis by a Rotaxane-Based Molecular Machine. *J. Am. Chem. Soc.* **2017**, *139*, 10875−10879.

(175) de Bo, G.; Gall, M. A. Y.; Kuschel, S.; De Winter, J.; Gerbaux, P.; Leigh, D. A. An Artificial Molecular Machine that Builds an Asymmetric Catalyst. *Nat. Nanotechnol.* **2018**, *13*, 381−385.

(176) McTernan, C. T.; de Bo, G.; Leigh, D. A. A Track-Based Molecular Synthesizer that Builds a Single-Sequence Oligomer through Iterative Carbon-Carbon Bond Formation. *Chem.* **2020**, *6*, 2964−2973.

(177) Berná, J.; Leigh, D. A.; Lubomska, M.; Mendoza, S. M.; Pérez, E. M.; Rudolf, P.; Teobaldi, G.; Zerbetto, F. Macroscopic Transport by Synthetic Molecular Machines. *Nat. Mater.* **2005**, *4*, 704−710.

(178) Chen, J.; Leung, F. K.-C.; Stuart, M. C. A.; Kajitani, T.; Fukushima, T.; van der Giessen, E.; Feringa, B. L. Artificial Muscle-Like Function from Hierarchical Supramolecular Assembly of Photoresponsive Molecular Motors. *Nat. Chem.* **2018**, *10*, 132−138.

(179) Lancia, F.; Ryabchun, A.; Katsonis, N. Life-Like Motion Driven by Artificial Molecular Machines. *Nat. Rev. Chem.* **2019**, *3*, 536−551.

(180) Shi, Z.-T.; Zhang, Q.; Tian, H.; Qu, D.-H. Driving Smart Molecular Systems by Artificial Molecular Machines. *Adv. Intell. Syst.* **2020**, *2*, 1900169.

(181) Liu, Y.; Flood, A. H.; Bonvallet, P. A.; Vignon, S. A.; Northrop, B. H.; Tseng, H.-R.; Jeppesen, J. O.; Huang, T. J.; Brough, B.; Baller, M.; Magonov, S.; Solares, S. D.; Goddard, W. A., III; Ho, C.-M.; Stoddart, J. F. Linear Artificial Molecular Muscles. *J. Am. Chem. Soc.* **2005**, *127*, 9745−9759.

(182) Juluri, B. K.; Kumar, A. S.; Liu, Y.; Ye, T.; Yang, Y.-W.; Flood, A. H.; Fang, L.; Stoddart, J. F.; Weiss, P. S.; Huang, T. J. A Mechanical Actuator Driven Electrochemically by Artificial Molecular Muscles. *ACS Nano* **2009**, *3*, 291−300.

(183) Kaleta, J.; Bastien, G.; Wen, J.; Dračínský, M.; Tortorici, E.; Císařová, I.; Beale, P. D.; Rogers, C. T.; Michl, J. Bulk Inclusions of Double Pyridazine Molecular Rotors in Hexagonal Tris(*o*-phenylene) Cyclotriphosphazene. *J. Org. Chem.* **2019**, *84*, 8449−8467.

(184) Kaleta, J.; Chen, J.; Bastien, G.; Dracinsky, M.; Masat, M.; Rogers, C. T.; Feringa, B. L.; Michl, J. Surface Inclusion of Unidirectional Molecular Motors in Hexagonal Tris(*o*-phenylene) Cyclotriphosphazene. *J. Am. Chem. Soc.* **2017**, *139*, 10486−10498.

(185) Ragazzon, G.; Prins, L. J. Energy Consumption in Chemical Fuel-Driven Self-Assembly. *Nat. Nanotechnol.* **2018**, *13*, 882−889.

(186) Vogelsberg, C. S.; Uribe-Romo, F. J.; Lipton, A. S.; Yang, S.; Houk, K. N.; Brown, S.; Garcia-Garibay, M. A. Ultrafast Rotation in an Amphidynamic Crystalline Metal Organic Framework. *Proc. Natl. Acad. Sci. U. S. A.* **2017**, *114*, 13613−13618.

(187) Howe, M. E.; Garcia-Garibay, M. A. The Roles of Intrinsic Barriers and Crystal Fluidity in Determining the Dynamics of Crystalline Molecular Rotors and Molecular Machines. *J. Org. Chem.* **2019**, *84*, 9835−9849.

(188) Deng, H.; Olson, M. A.; Stoddart, J. F.; Yaghi, O. M. Robust Dynamics. *Nat. Chem.* **2010**, *2*, 439−443.

(189) Chen, Q.; Sun, J.; Li, P.; Hod, I.; Moghadam, P. Z.; Kean, Z. S.; Snurr, R. Q.; Hupp, J. T.; Farha, O. K.; Stoddart, J. F. A Redox-Active Bistable Molecular Switch Mounted inside a Metal-Organic Framework. *J. Am. Chem. Soc.* **2016**, *138*, 14242−14245.

(190) Jiang, X.; Duan, H.-B.; Khan, S. I.; Garcia-Garibay, M. A. Diffusion-Controlled Rotation of Triptycene in a Metal-Organic Framework (MOF) Sheds Light on the Viscosity of MOF-Confined Solvent. *ACS Cent. Sci.* **2016**, *2*, 608−613.

(191) Vukotic, V. N.; Harris, K. J.; Zhu, K.; Schurko, R. W.; Loeb, S. J. Metal-Organic Frameworks with Dynamic Interlocked Components. *Nat. Chem.* **2012**, *4*, 456−460.

(192) Zhu, K.; Vukotic, V. N.; O'Keefe, C. A.; Schurko, R. W.; Loeb, S. J. Metal-Organic Frameworks with Mechanically Interlocked Pillars: Controlling Ring Dynamics in the Solid-State via a Reversible Phase Change. *J. Am. Chem. Soc.* **2014**, *136*, 7403−7409.

(193) Zhu, K.; O'Keefe, C. A.; Vukotic, V. N.; Schurko, R. W.; Loeb, S. J. A Molecular Shuttle that Operates inside a Metal-Organic Framework. *Nat. Chem.* **2015**, *7*, 514−519.

(194) Martinez-Bulit, P.; Stirk, A. J.; Loeb, S. J. Rotors, Motors, and Machines inside Metal-Organic Frameworks. *Trends Chem.* **2019**, *1*, 588−600.

(195) Wilson, B. H.; Loeb, S. J. Integrating the Mechanical Bond into Metal-Organic Frameworks. *Chem.* **2020**, *6*, 1604−1612.

(196) Wilson, B. H.; Vojvodin, C. S.; Gholami, G.; Abdulla, L. M.; O'Keefe, C. A.; Schurko, R. W.; Loeb, S. J. Precise Spatial Arrangement and Interaction between Two Different Mobile Components in a Metal-Organic Framework. *Chem* **2020**, *7*, 202−211.

(197) Terzopoulou, A.; Nicholas, J. D.; Chen, X.-Z.; Nelson, B. J.; Pané, S.; Puigmartí-Luis, J. Metal-Organic Frameworks in Motion. *Chem. Rev.* **2020**, *120*, 11175−11193.

(198) Collier, C. P.; Mattersteig, G.; Wong, E. W.; Luo, Y.; Beverly, K.; Sampaio, J.; Raymo, F. M.; Stoddart, J. F.; Heath, J. R. A [2]Catenane-Based Solid State Electronically Reconfigurable Switch. *Science* **2000**, *289*, 1172−1175.

(199) Collier, C. P.; Jeppesen, J. O.; Luo, Y.; Perkins, J.; Wong, E. W.; Heath, J. R.; Stoddart, J. F. Molecular-Based Electronically Switchable Tunnel Junction Devices. *J. Am. Chem. Soc.* **2001**, *123*, 12632−12641.

(200) Luo, Y.; Collier, C. P.; Jeppesen, J. O.; Nielsen, K. A.; DeIonno, E.; Ho, G.; Perkins, J.; Tseng, H.-R.; Yamamoto, T.;

Stoddart, J. F.; Heath, J. R. Two-Dimensional Molecular Electronics Circuits. *ChemPhysChem* **2002**, *3*, 519−525.

(201) Green, J. E.; Choi, J. W.; Boukai, A.; Bunimovich, Y.; Johnston-Halperin, E.; DeIonno, E.; Luo, Y.; Sheriff, B. A.; Xu, K.; Shik Shin, Y.; Tseng, H.-R.; Stoddart, J. F.; Heath, J. R. A 160-Kilobit Molecular Electronic Memory Patterned at 10^{11} Bits per Square Centimetre. *Nature* **2007**, *445*, 414−417.

(202) Eelkema, J. J. R.; Pollard, M. M.; Vicario, J.; Katsonis, N.; Serrano Ramon, B.; Bastiaansen, C. W. M.; Broer, D. J.; Feringa, B. L. Nanomotor Rotates Microscale Objects. *Nature* **2006**, *440*, 163.

(203) Flood, A. H.; Peters, A. J.; Vignon, S. A.; Steuerman, D. W.; Tseng, H.-R.; Kang, S.; Heath, J. R.; Stoddart, J. F. The Role of Physical Environment on Molecular Electromechanical Switching. *Chem. - Eur. J.* **2004**, *10*, 6558−6564.

(204) Choi, J. W.; Flood, A. H.; Steuerman, D. W.; Nygaard, S.; Braunschweig, A. B.; Moonen, N. N. P.; Laursen, B. W.; Luo, Y.; DeIonno, E.; Peters, A. J.; Jeppesen, J. O.; Xu, K.; Stoddart, J. F.; Heath, J. R. Ground-State Equilibrium Thermodynamics and Switching Kinetics of Bistable [2]Rotaxanes Switched in Solution, Polymer Gels, and Molecular Electronic Devices. *Chem. - Eur. J.* **2006**, *12*, 261−279.

(205) Li, Q.; Fuks, G.; Moulin, E.; Maaloum, M.; Rawiso, M.; Kulic, I.; Foy, J. T.; Giuseppone, N. Macroscopic Contraction of a Gel Induced by the Integrated Motion of Light-Driven Molecular Motors. *Nat. Nanotechnol.* **2015**, *10*, 161−165.

(206) Foy, J. T.; Li, Q.; Goujon, A.; Colard-Itté, J. R.; Fuks, G.; Moulin, E.; Schiffmann, O.; Dattler, D.; Funeriu, D. P.; Giuseppone, N. Dual-Light Control of Nanomachines that Integrate Motor and Modulator Subunits. *Nat. Nanotechnol.* **2017**, *12*, 540−545.

(207) Colard-Itté, J. R.; Li, Q.; Collin, D.; Mariani, G.; Fuks, G.; Moulin, E.; Buhler, E.; Giuseppone, N. Mechanical Behaviour of Contractile Gels Based on Light-Driven Molecular Motors. *Nanoscale* **2019**, *11*, 5197−5202.

(208) Mariani, G.; Colard-Itté, J. R.; Moulin, E.; Giuseppone, N.; Buhler, E. Structural Properties of Contractile Gels Based on Light-Driven Molecular Motors: A Small-Angle Neutron and X-Ray Study. *Soft Matter* **2020**, *16*, 4008−4023.

(209) Moulin, E.; Faour, L.; Carmona-Vargas, C. C.; Giuseppone, N. From Molecular Machines to Stimuli-Responsive Materials. *Adv. Mater.* **2020**, *32*, 1906036.

(210) Dattler, D.; Fuks, G.; Heiser, J.; Moulin, E.; Perrot, A.; Yao, X.; Giuseppone, N. Design of Collective Motions from Synthetic Molecular Switches, Rotors, and Motors. *Chem. Rev.* **2020**, *120*, 310−433.

(211) Boyle, M. M.; Smaldone, R. A.; Whalley, A. C.; Ambrogio, M. W.; Botros, Y. Y.; Stoddart, J. F. Mechanised Materials. *Chem. Sci.* **2011**, *2*, 204−210.

(212) García-López, V.; Chen, F.; Nilewski, L. G.; Duret, G.; Aliyan, A.; Kolomeisky, A. B.; Robinson, J. T.; Wang, G.; Pal, R.; Tour, J. M. Molecular Machines Open Cell Membranes. *Nature* **2017**, *548*, 567−572.

(213) García-López, V.; Liu, D.; Tour, J. M. Light-Activated Organic Molecular Motors and their Applications. *Chem. Rev.* **2020**, *120*, 79−124.